TECHNICAL REPORT STANDARD TITLE PAGE

1. Report No.	2. Government Accession No.	3. Recipient's Catalog No.
FHWA/TX-81/38+247-2		

4. Title and Subtitle	5. Report Date
FIELD TESTS OF A CONTINUOUS TWIN GIRDER STEEL BRIDGE	November 1981
	6. Performing Organization Code
7. Author(s)	8. Performing Organization Report No.
J. A. Yura, K. H. Frank, and A. K. Gupta	Research Report 247-2
9. Performing Organization Name and Address	10. Work Unit No.
Center for Transportation Research The University of Texas at Austin Austin, Texas 78712	11. Contract or Grant No. Research Study 3-5-79-247
	13. Type of Report and Period Covered
12. Sponsoring Agency Name and Address Texas State Department of Highways and Public Transportation; Transportation Planning Division P. O. Box 5051 Austin, Texas 78763	Interim
	14. Sponsoring Agency Code

15. Supplementary Notes

Study conducted in cooperation with the U. S. Department of Transportation, Federal Highway Administration. Research Study Title: "Evaluation of the Fatigue Life of Structural Steel Bridge Details"

16. Abstract

The structural behavior of a twin girder continuous steel bridge was studied in the field to provide data for a fatigue evaluation of the structure. Girder strains and deflections were measured under normal traffic and with a 52,000-lb test truck traveling at various speeds up to 50 mph using high-speed data acquisition equipment.

An analysis of the data showed a maximum flange stress range of 3.1 ksi due to the test truck. A structural analysis of the bridge gave theoretical results which were within 10 percent of the measured flange stresses. Experimental data with the truck at high speed were more reliable than data with the truck stationary.

17. Key Words	18. Distribution Statement
steel bridge, continuous twin girder, field tests, structural behavior, fatigue evaluator, strains, deflections	No restrictions. This document is available to the public through the National Technical Information Service, Springfield, Virginia 22161.

19. Security Classif. (of this report)	20. Security Classif. (of this page)	21. No. of Pages	22. Price
Unclassified	Unclassified	126	

Form DOT F 1700.7 (8-69)

FIELD TESTS OF A CONTINUOUS TWIN GIRDER STEEL BRIDGE

by

J. A. Yura
K. H. Frank
A. K. Gupta

Research Report Number 247-2

Evaluation of the Fatigue Life of
Structural Steel Bridge Details

Research Project 3-5-79-247

conducted for

Texas
State Department of Highways and Public Transportation

in cooperation with the
U. S. Department of Transportation
Federal Highway Administration

by the

CENTER FOR TRANSPORTATION RESEARCH
BUREAU OF ENGINEERING RESEARCH
THE UNIVERSITY OF TEXAS AT AUSTIN

November 1981

The contents of this report reflect the views of the authors, who are responsible for the facts and the accuracy of the data presented herein. The contents do not necessarily reflect the official views or policies of the Federal Highway Administration. This report does not constitute a standard, specification, or regulation.

A C K N O W L E D G E M E N T S

A. Leite and D. Platten, graduate students at The University of Texas at Austin, contributed significantly to the planning, data collection and data reduction for the research program.

The field tests were conducted with the help of the staff of Ferguson Structural Engineering Laboratory and the Texas State Department of Highways and Public Transportation, Dallas Division, whose help is gratefully acknowledged.

A B S T R A C T

The structural behavior of a twin girder continuous steel bridge was studied in the field to provide data for a fatigue evaluation of the structure. Girder strains and deflections were measured under normal traffic and with a 52,000-lb test truck traveling at various speeds up to 50 mph using high-speed data acquisition equipment.

An analysis of the data showed a maximum flange stress range of 3.1 ksi due to the test truck. A structural analysis of the bridge gave theoretical results which were within 10% of the measured flange stresses. Experimental data with the truck at high speed were more reliable than data with the truck stationary.

TABLE OF CONTENTS

LIST OF FIGURES

CHAPTER 1

INTRODUCTION

It has been estimated that there are more than half a million highway and railroad bridges in the United States. With only a few exceptions, these structures have performed satisfactorily in every respect [2]. Of the failures that have occurred, many have been due to fractures initiated by fatigue. These failures have led to a better understanding of bridge fatigue behavior [5]. As has been pointed out by Fisher in his Bridge fatigue guide [2], welding and welded details have a large influence on the life expectancy of highway bridges. The primary variables influencing fatigue strength are the type of detail, the stress range to which the detail is subjected and the frequency of occurrence of the stress cycles. Fatigue crack initiation and growth is influenced, not by the actual maximum stress, but, by the fluctuation of stress, i.e., the stress range. Once a crack has been initiated, and the type of loading acting on it is known, the number of cycles of stress before failure can be estimated from laboratory tests on various welded and bolted details. Fatigue specifications [3] published by AASHTO (American Association of State Highway and Transportation Officials) divide bridge details into seven categories according to their severity. Category A is the best while category E' is the worst. Some of these details are shown in Fig. 1.1. As shown in Fig. 1.1a, the welded flange transition under tension is a category C detail, but when ground flush it improves to category B. The welded web and flange joint is a category B detail. In Fig. 1.1b, the end of any welded longitudinal web stiffner is a category E detail, one of the worst possible. Further away from the end of the stiffner, the detail improves to category B. Hence the severity

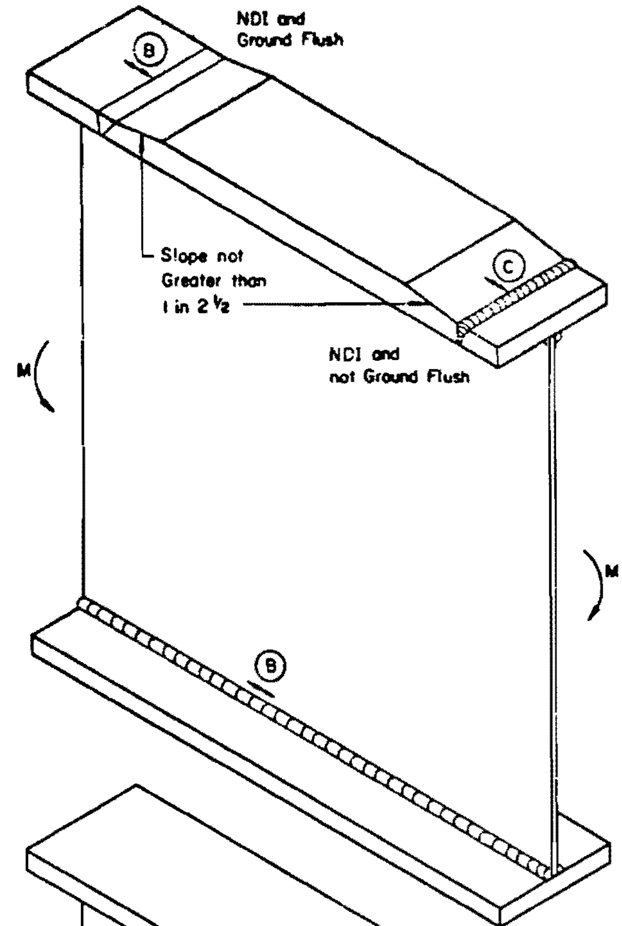

Fig. 1.1(a)

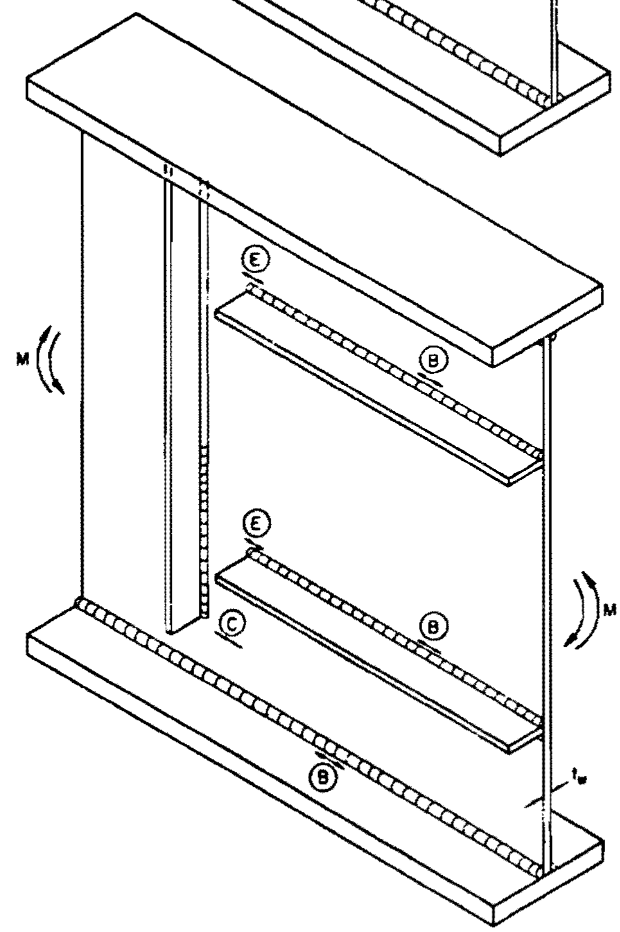

Fig. 1.1(b)

of any bridge detail can be determined reasonably well by classification of the detail into an appropriate category. The actual stress range and the frequency of that stress range to which the detail is subjected must be established by the designer in order to calculate the fatigue life.

Due to the basic assumptions made in the design process, calculated design stresses tend to be generally conservative. Field tests have shown that the actual stresses in a structure are generally smaller than calculated by the designer [2]. In the fatigue specifications, a factor Alpha has been used to represent the ratio of the actual stress range due to the passage of a design vehicle to the calculated design stress range. According to Fisher, conservative values of Alpha of about 0.8 for transverse members and 0.7 for longitudinal members were determined from field tests and used to derive the ADTT (Average Daily Truck Traffic) found in the AASHTO specifications.

A graphical representation of the AASHTO fatigue specification is shown in Fig. 1.2. When using the specification, the stress range is based on the design calculations; the alpha factor has already been incorporated in the recommendations. As standard structural analysis becomes more sophisticated using computer programs which account for the three dimensional response of the structure including the effects of the bridge deck and the bracing members, the alpha adjustment incorporated in the AASHTO specifications [2] may be unwarranted and unconservative. The importance of an accurate evaluation of the stress range is shown in Fig. 1.2. A reduction in the stress fluctuation of 10% increases the number of cycles to failure by 25%. In other words, an underestimation of the stress range by 10% will overestimate the life expectancy by 25%. If the fatigue life is to be reliably evaluated for an existing structure, field tests may be necessary to determine the stress range.

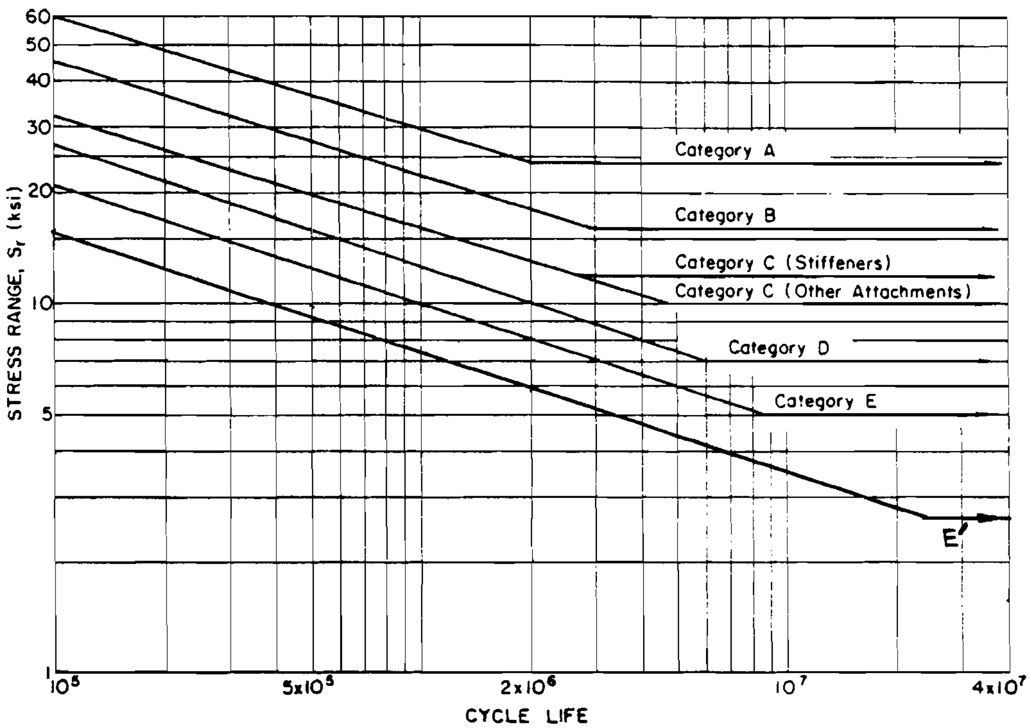

Fig. 1.2 Design stress range curves for Categories A to E′ (from Ref 2)

Many steel bridges in Texas were designed before the present fatigue provisions were incorporated into the bridge specifications. Hence they have details which may not satisfy the AASHTO fatigue resistance requirements for fracture critical members, or they may contain details which have not been tested and categorized. Very few incidents of fatigue cracking have been noticed to date, but some problems may become evident as the number of stress cycles increases. Even more so, the bridges in Texas are generally not too old, therefore they have been subjected to a small number of stress cycles of their total stress life. Also, as years go by, these bridges are subjected to more and more overloads. For example, the existing international bridge in Laredo, Texas, has a long history of overloads, which has caused some structural damage. In a 10-month period it experienced over 3,750 overloads ranging from 72,000 to 120,000 lbs [4]. When overloadings occur with such regularity, they can no longer be classified as infrequent loadings. Since these documented overloads were based on a study of permit applications, it would be expected that even more actual overloads occurred. They all tend to reduce the fatigue life of severe details.

The general objective of the project is the determination of the fatigue life of a series of continuous twin girder bridges used in an interstate exchange in Dallas. The bridges are 72 in deep steel plate girders with intersecting cross beams spaced approximately 20 ft on center, as shown in Fig. 1.3a. These bridges have some special characteristics that make them different from the bridges normally encountered. Since only two girders support the structure, the system would collapse even if fracture occurs in one girder only. Hence, the twin girder arrangement makes the system fracture critical. The 48 in deep crossbeams, shown in Fig. 1.3b, are very deep compared to those

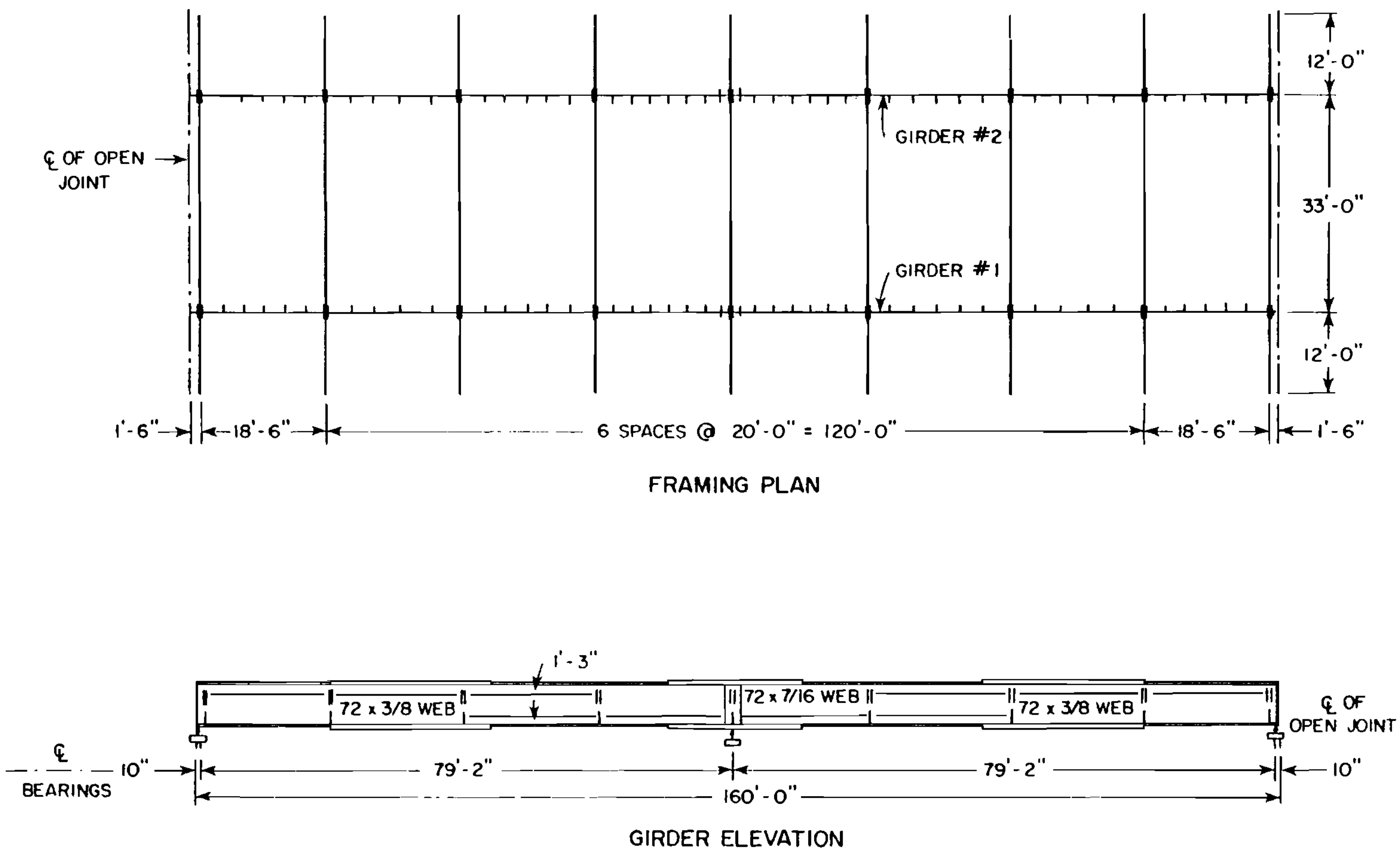

Fig. 1.3a Typical plan and elevation of a continuous twin girder bridge

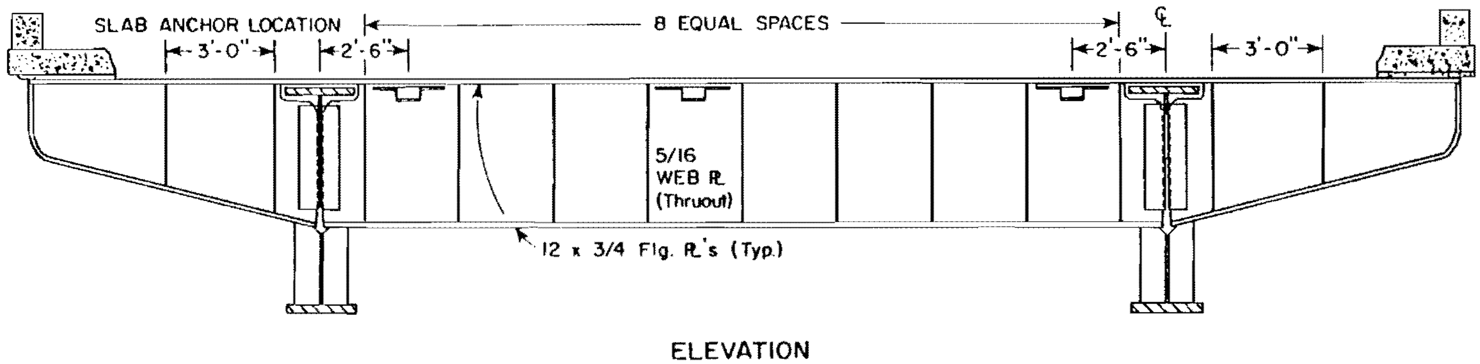

Fig. 1.3b Typical elevation of a crossbeam with connected deck

generally found in other bridges. The girders are not connected by a bottom lateral system or other diaphragms. Some of the girders are suspended at the end by hanger plates. The cross-beams support a post-tensioned concrete deck, 10.5 in thick which is connected to the crossbeams with bolts at discrete points. The slab is not in contact with the girder. The vehicle load is transmitted through the crossbeams to the girders.

The 72 in deep main girders have both transverse and longitudinal stiffners which introduce a significant number of possible sites of fatigue cracking within the span. The flange plate thickness is increased from 1-1/4 in to 1-3/4 in near the support. This flange splice is a category B detail as seen in Fig. 1.1a. The horizontal stiffners end before they reach the vertical stiffners. This detail is normally a category E, as shown in Fig. 1.1b. However, due to the small gap between the two stiffners, 1/2 in, the detail may be more severe.

The specific objective of this thesis is to study the structural behavior of the bridges mentioned above. Stress range, an important variable in fatigue life determination, is measured in the field under static and dynamic loads. Field data is compared with the analytical solution in order to verify and calibrate the analytical assumptions in design. The distribution of load between the two girders is considered. In other theses, the flange splice and the stiffner end detail has been studied in depth so as to establish the fatigue behavior of these details.

CHAPTER 2

FIELD TESTING

2.1 Test Span Location

The bridge system under study is a part of the IH345 and IH20 expressway intersection near the downtown Dallas area. It stretches over a distance of many miles and is an intricate elevated interchange. It consists mainly of twin girder steel bridges with post-tensioned concrete decks, as shown in Fig. 2.1.

The particular structure chosen for the field testing, designated as structure F18S on the Texas Highway Department roadway plans, is shown in Fig. 2.2. It is a five span bridge that is symmetric about the centerline of the roadway. Both the web and the flanges change in thickness near the supports. The flange plates are 24" × 1-1/4" in the middle of the span and they increase in thickness to 1-3/4" near the interior support. The web plate is 72" deep and 3/8" thick. It has both vertical and horizontal stiffeners attached to it.

The test structure is adjacent to the entrance ramp shown in Fig. 2.3. Various factors that were considered in choosing this five span bridge from the vast number of available structures on the expressway, are listed below.

(1) The test-span has a horizontal curve of only three degrees. This would facilitate the structural analysis of the bridge at a later stage.

(2) The absence of entrance and exit ramps makes it easy to close a lane on the bridge if needed.

(3) The large area of compacted ground under the test-span is free of any intersecting roads, thus making it easy to

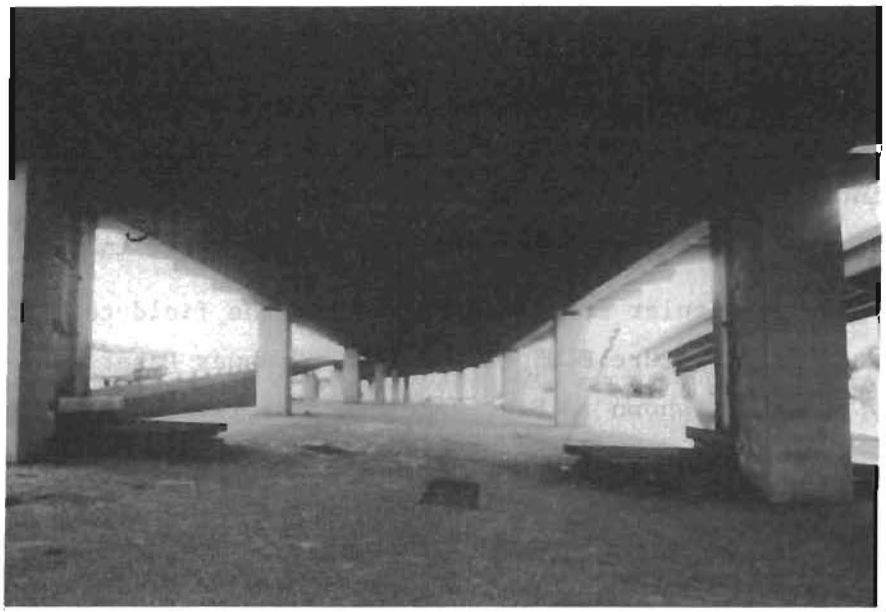

Fig. 2.1 Underview of a twin girder steel bridge

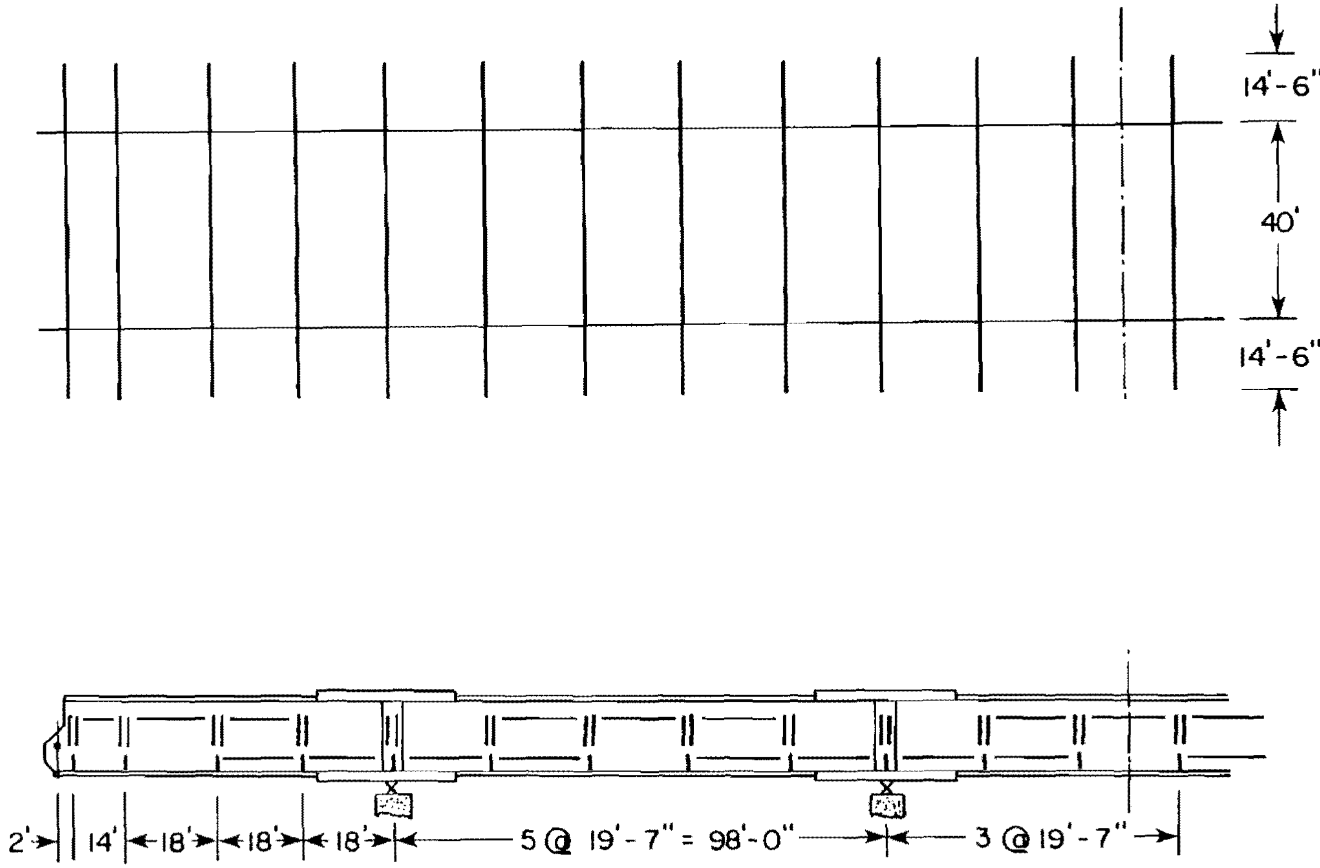

Fig. 2.2 Structure F185, symmetric about centerline

Fig. 2.3 Structure F185, photograph

work under and place instrument vans. Also the area is easily accessible by road, facilitating the transportation of delicate data recording equipment into position.

(4) The span is about 18 feet above the ground, making it reasonably easy to attach the instrumentation.

(5) One end of the span is suspended by hanger plates to simulate a pinned joint. These hanger plates, as shown in Fig. 2.4, are suspended from a box beam. In the past, one of these hanger support details experienced a fatigue failure, but the problem was assumed to have resulted from a fabrication omission.

(6) There have been reports of excessive vibration near the hanger support in this span.

2.2 Instrumentation

The bridge consists of two steel girders, both of which were instrumented with strain gages as shown in Fig. 2.5. The hanger plates were strain-gaged to determine reaction at the support. Strain gages were also placed at two locations near the center of the first span to find the moments in the girder. Two locations were chosen to provide an independent check of the results. Both the girders were instrumented, to find the distribution of load between them.

The hanger support consists of two hanger plates. Figure 2.6 shows the location of the four gages that were used at each support. Both hangers were gaged to measure the possible unequal distribution of load among the two plates caused by torsion or eccentricity in the girder. The two gages were placed, on opposite edges, to account for the in-plane bending of the hanger plate due to friction at the pins. The average of these four gages provided a reasonably good estimate of the reaction.

As shown in Fig. 2.7, both flange plates were instrumented at the location where the girder moment was to be determined. The

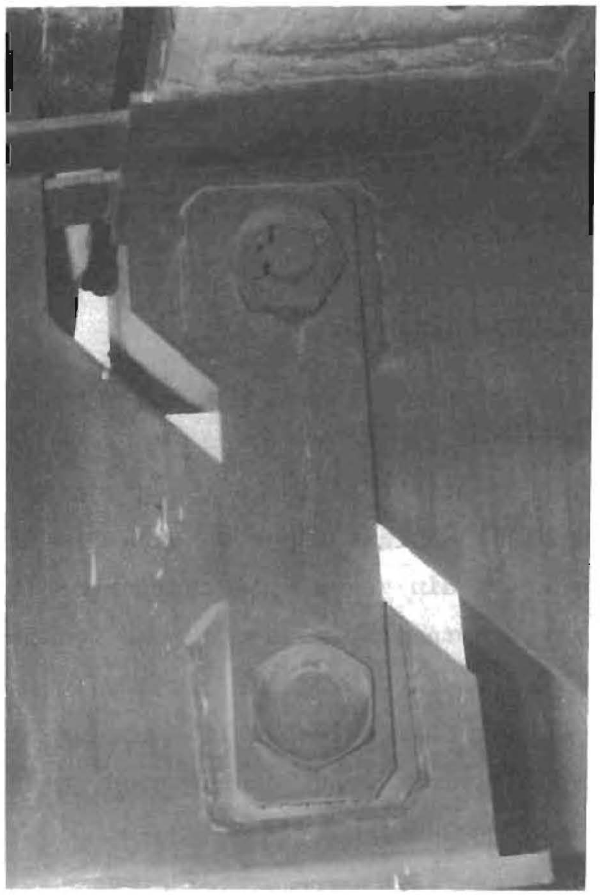

Fig. 2.4a Hanger support in field

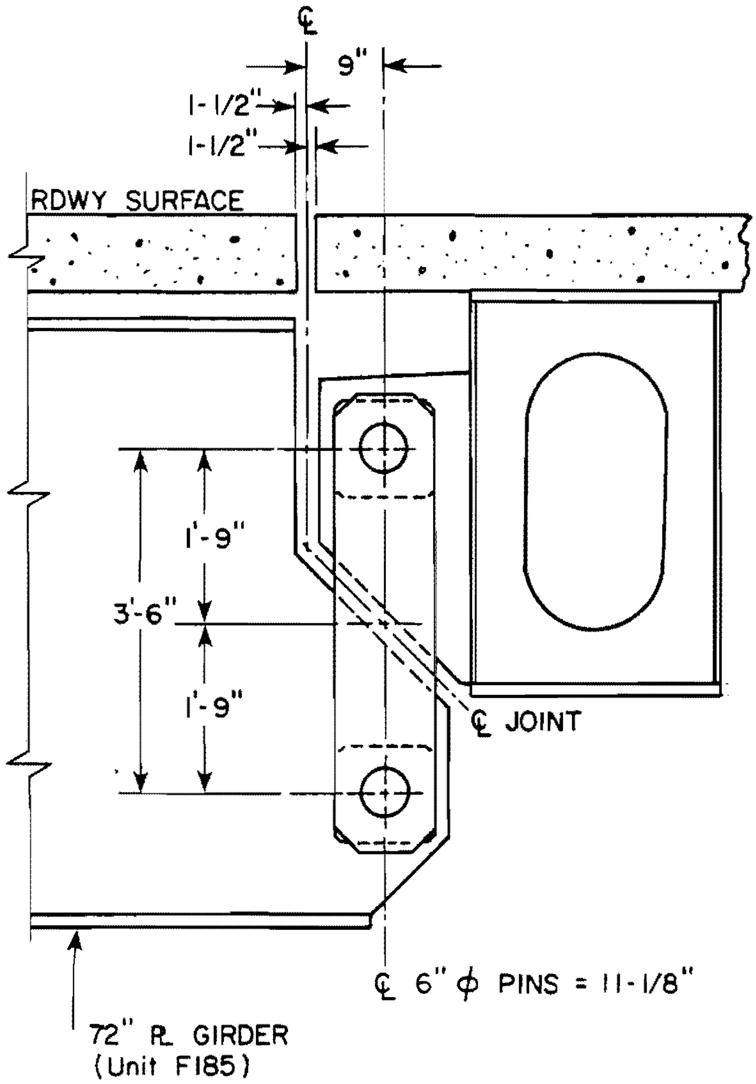

Fig. 2.4b Hanger support detail

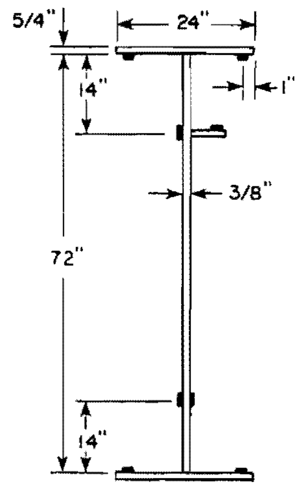

Fig. 2.5 Gaged sections on F18S

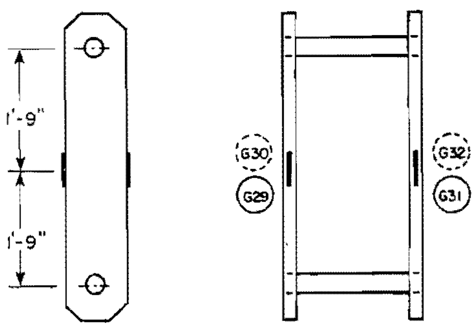

Fig. 2.6 Hanger plate gages

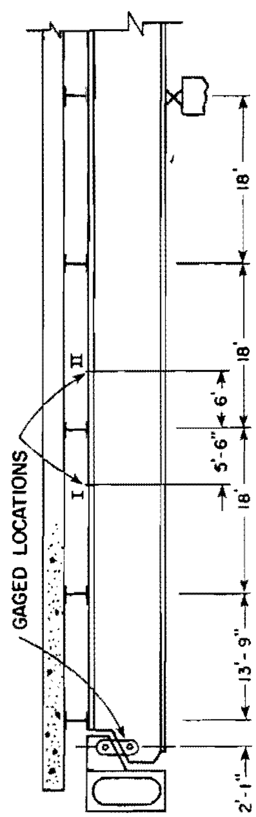

Fig. 2.7 Strain gages at Locations I & II

stresses in the two flanges could be used to establish if any composite action develops between the girder and the slab. A gage was placed an inch away from the edge of each flange. These gages were placed on the inside surface of the flanges because the extreme fiber was not accessible due to the presence of the deck slab as shown in Fig. 2.8 (Gage D19). In the initial tests some gages were also placed on the web to establish if plane sections remain plane. These web gages were placed near the quarter point of the web, like gage D23 in Fig. 2.8. Strain gages were also used to establish the stress distribution along the length of a longitudinal stiffener and near its termination at a transverse stiffener. The location of these "stiffener" gages and their results are presented elsewhere. (Ref.--Platten)

Two moment locations were chosen near the center of the first span, where analysis indicated the moments were the largest. As shown in Fig. 2.5, they were located a distance approximately equal to the depth of the girder, away from a cross-beam, to ensure that the local stresses due to the cross-beam were minimal.

2.3 Deflection Gages

Cantilever-type deflection gages, as shown in Fig. 2.9, were used to measure the deflection at one moment location on each girder. They consist of triangular aluminum plates stiffened at the base. The base is clamped to the flange of the girder where the deflection is to be measured. The gage then protrudes from the flange like a cantilever with a piano wire attached to the apex of the triangle which extends to the ground. The wire is anchored to the ground and tensioned to produce a cantilever gage deflection greater than the anticipated bridge deflection. As the bridge deflects, the tension in the wire reduces and the resulting bending strain in the cantilever is measured by the strain gages. These strain measurements are calibrated to the

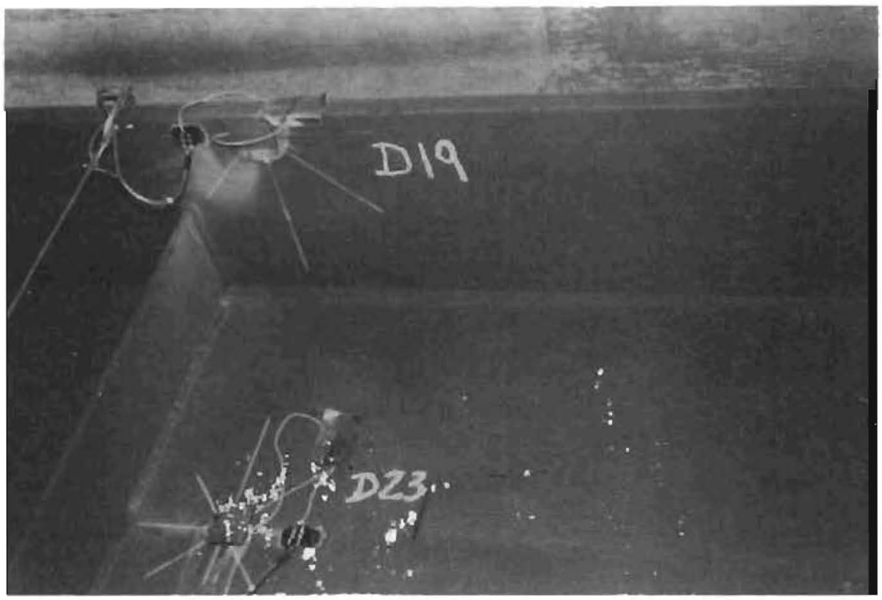

Fig. 2.8 Location of gages D19 & D23

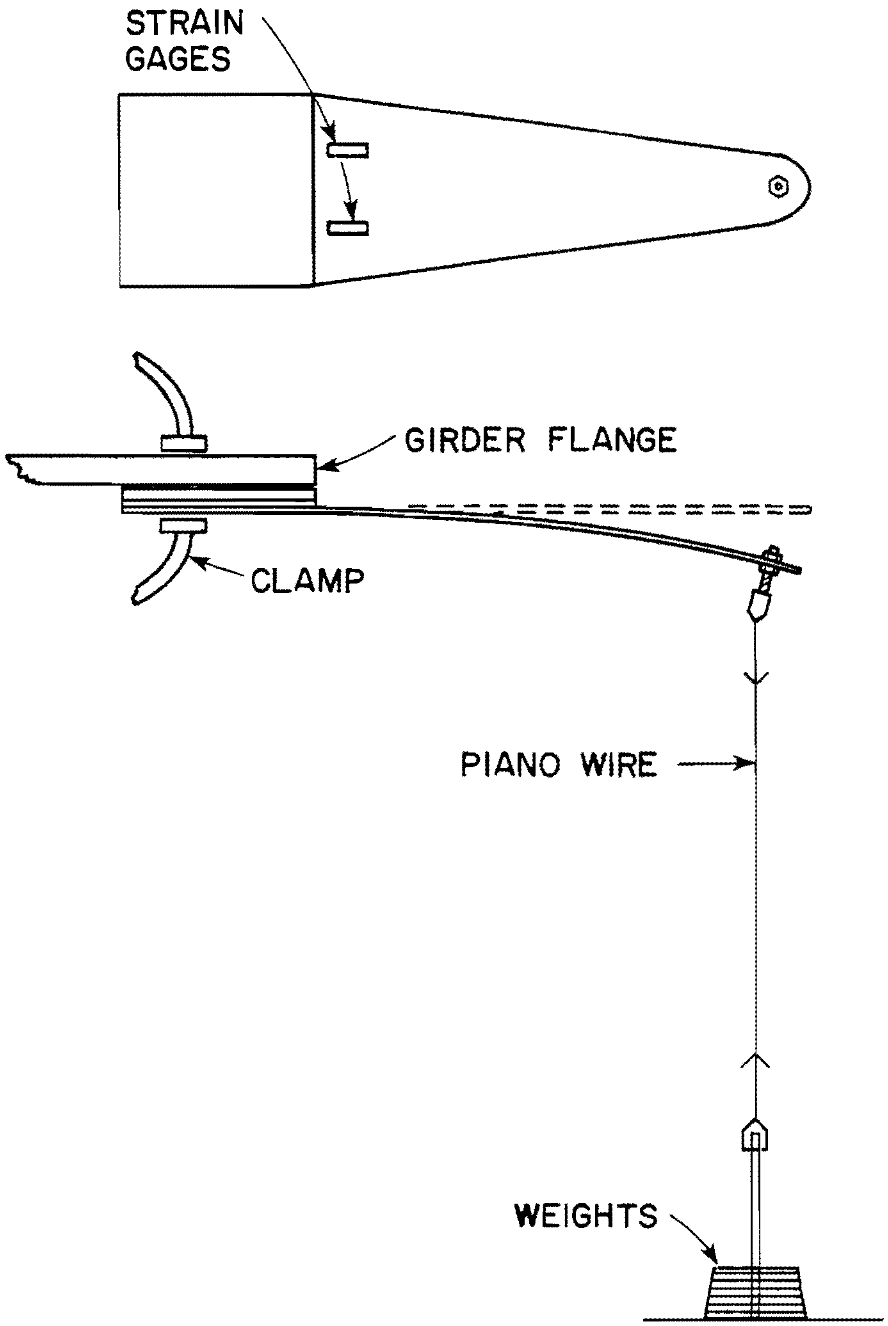

Fig. 2.9 Deflection gage

deflection as shown in Appendix A. The initial tension in the wire has no effect on the ratio of the strain measurements to the bridge deflection as shown in Appendix A. Fig. 2.10 shows two deflection gages placed on the opposite edges of the flange to measure girder deflection and rotation.

2.4 Strain-gaging

A lift-bucket, as shown in Fig. 2.11, and scaffolding were used to reach the steel structure. The locations to be gaged were measured off and marked. An electric grinder was used to remove the paint and to smooth the metal surface at each gage location. The metal surface was cleaned with Acetone and a mild acid was then applied to etch and condition the metal. A base was applied to neutralize the remaining acid. Eastman-910 cement was used to attach the gage to the prepared metal surface.

Strain gages number EA-06-250BG-120, marketed by Micro-Measurements (MM), were used. These 120 ohm gages are self temperature compensating when used on structural steel. The gage is .250 in. long and 0.125 in. wide. The gage was waterproofed using a Barrier-B liquid and as a further protection the gage was covered with a Barrier-E black mastik.

The two wires from the gage were connected to a terminal block glued to the structure adjacent to the gage. A three strand wire system which compensates for any temperature effect on the wire (Ref. B), completed the circuit to the data acquisition system. The gage and the terminal block were left in position on the bridge permanently, while the connector wire was removed after the tests.

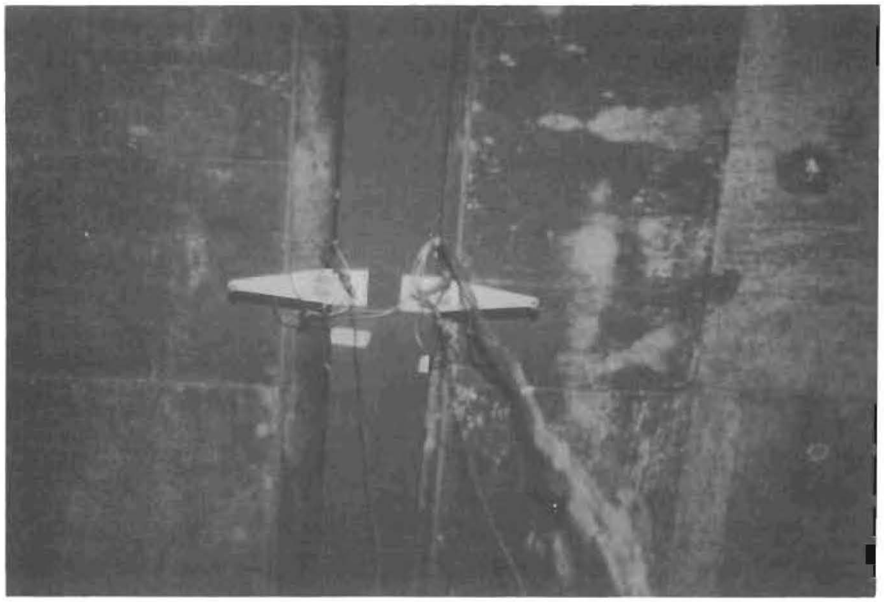

Fig. 2.10 Deflection gages as mounted

Fig. 2.11 A lift bucket, reaching up

2.5 Data Acquisition

A Vidar high speed digital data acquisition system, as shown in Fig. 2.12, was used to collect and store the data in the field. The system sequentially scans upto 96 channels of information, converting analog data into binary codes, for recording on magnetic tape. Later a high speed computer is utilized to reduce the recorded binary code to engineering units. At the time of the tests, only 40 of the available 96 channels of the Vidar system were operational. Channel 0 was used to monitor the bridge voltage, while channels 1 through 39 were set up to accept strain gage and deflection gage input.

The system is capable of operating in either of two modes. In Mode 1, a single scan of all channels is performed each time the system is started manually. In Mode 2, the system scans all channels continuously. An electronic timing device is utilized to establish the time interval between scans when the system is operated in Mode 2. The system was used in both modes during the test. The time required to scan the 40 channels was 0.004 seconds. The time interval between scans was varied from 0.1 seconds for the crawl speed truck tests to 0.06 seconds for the 50 mph tests.

2.6 Truck Selection

A structural analysis indicated that the maximum flexural stress range increased as the truck-wheel-base was reduced. The maximum stress range also increased as the weight of the truck increased. Hence a test truck with a small wheel-base coupled with a large load would produce the largest stress range. Since trucks with small wheel-bases usually have lower load capacities than those with longer bases, a number of trucks shown in Fig. 2.13 which were available for use on the bridge were considered. The truck shown in Fig. 2.14 was used as the test truck. The test

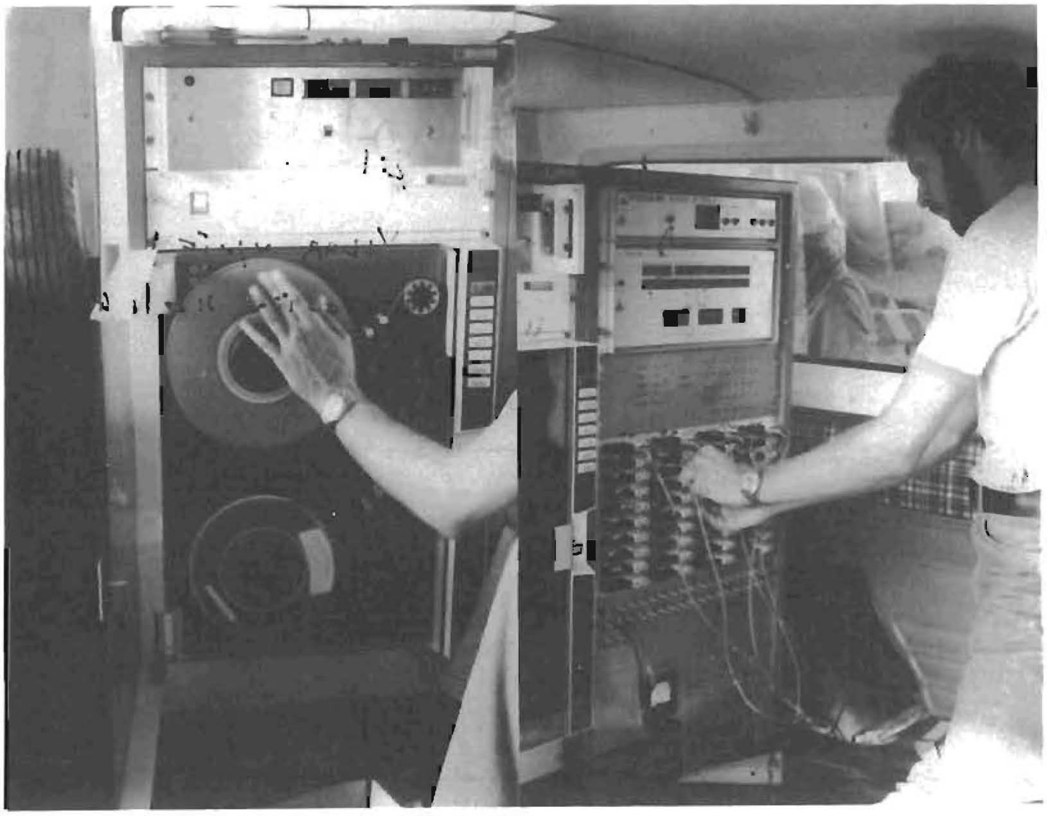

Fig. 2.12 High speed digital data acquisition system

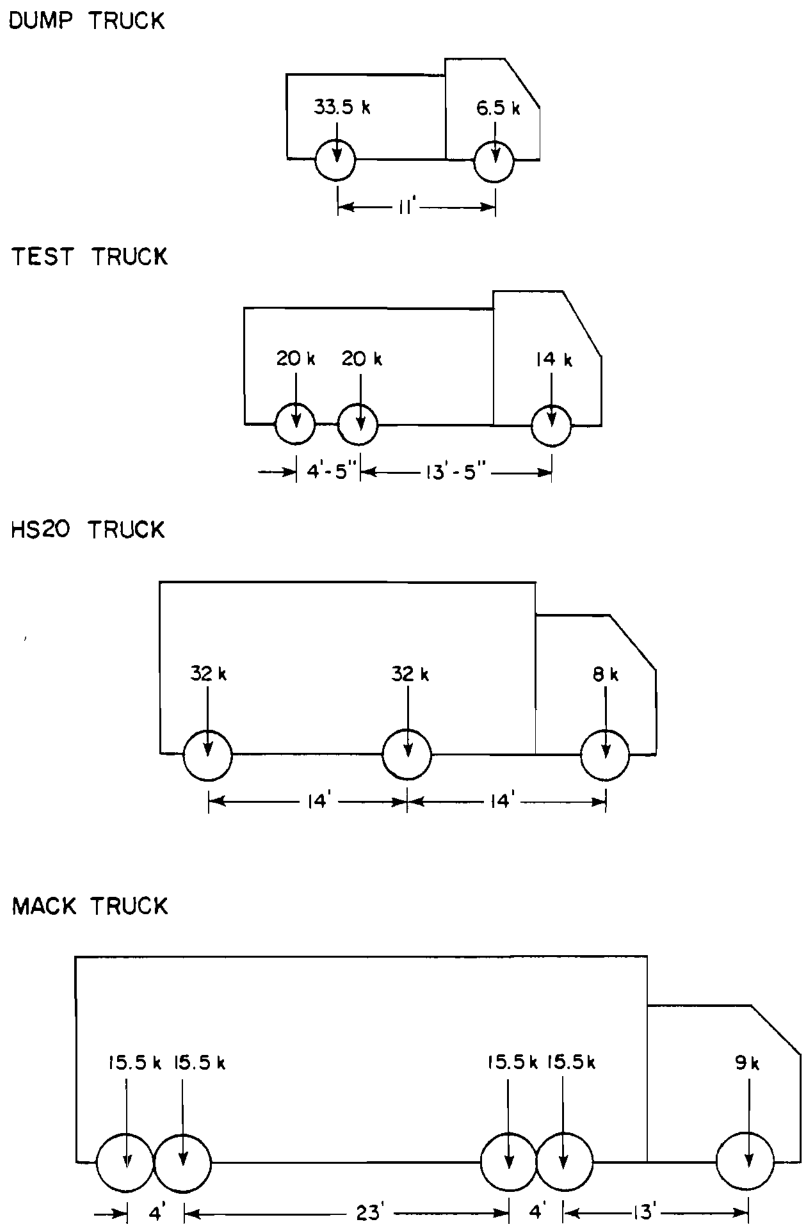

Fig. 2.13 Various trucks considered

Fig. 2.14 Test truck on structure F185

truck produces a maximum stress range larger than that produced by a Mack truck, although the Mack truck weighs much more, as shown in Table 2.1. For comparison, the maximum stress produced by the AASHTO design truck, HS20, is also shown.

TABLE 2.1

Truck	Weight (kips)	Maximum Stress (ksi)
Dump	40	3.4
Mack	71	4.0
HS20	72	5.3
Test	55	4.3

2.7 Field Procedure

Two separate field tests were conducted on the test span. The first field test was conducted on the 13th and 14th of July, 1979, when temperatures had reached 100 degrees F. In addition to the discomfort, this high temperature also created problems in the Vidar system on the first day due to the excessive heat. On the second day the doors of the van, where the Vidar was housed, were opened and air circulation was utilized to cool the Vidar.

Two types of runs were made during the field tests; static load cases and dynamic runs. From an analytical study, a truck location was found that would produce the maximum stress range at each of the gaged sections. The resultant truckload was placed at these two locations in the first span, i.e. positions B and C, as shown in Fig. 2.15. The truck was centered directly over one of the girders as shown in Fig. 2.16, thus producing the largest possible stress in that girder. A large stress range was necessary to reduce the ratio of the switching error in the gage

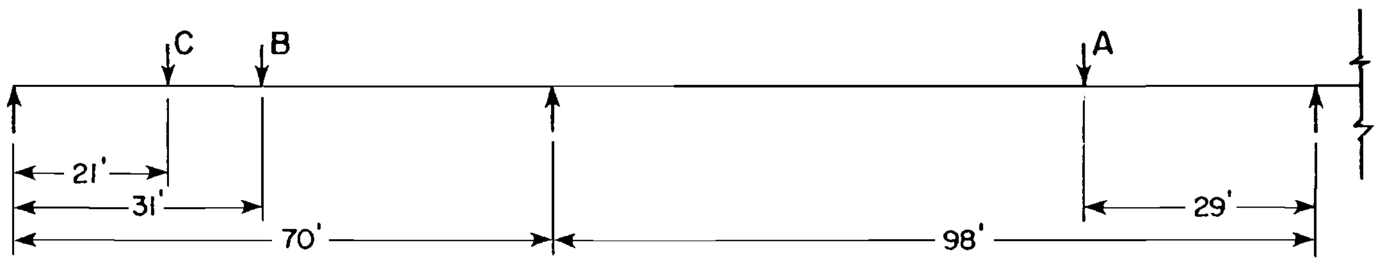

Fig. 2.15 3 Static truck Locations

(Position of the resultant truck load is shown)

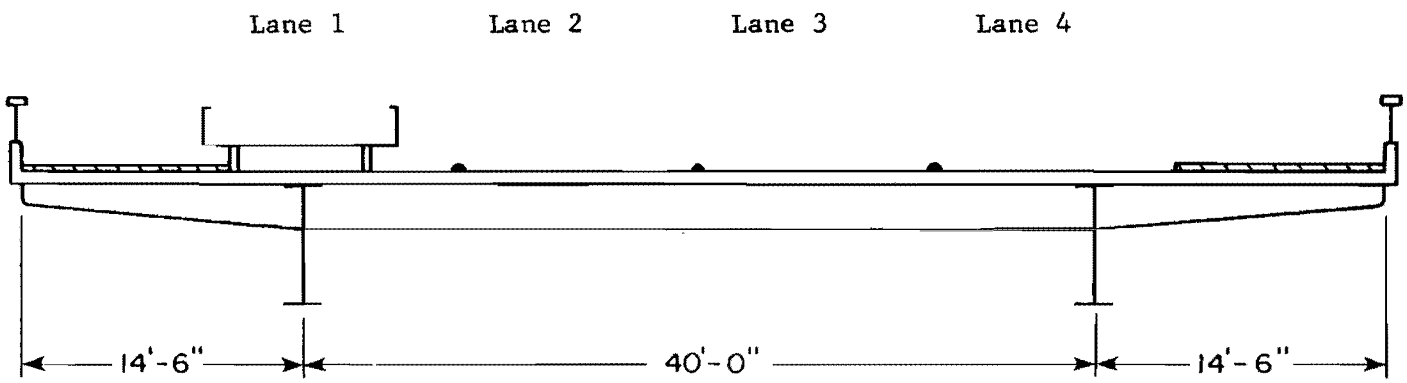

Fig. 2.16 Truck location across the bridge

readings, thereby increasing the reliability of the data. One static location was also chosen on the second span at position A, to get negative moment readings from the gages. Mode 1 of the Vidar System was used to record the data. Five data scans were made at each truck location. Two static runs were made to produce replicate data. Levels 1 and 2 were closed to normal traffic (Fig 2.17).

The dynamic runs were made with the truck centered over one of the girders, again to get the largest possible stress. Mode 2 of the Vidar system was used to record the dynamic data.

Dynamic runs were made at approximately 5 mph and 30 mph. Replicate data was taken for each type of run. The truck was accelerated to its velocity before it reached the instrumental span, and then driven at a reasonably constant speed. The normal traffic on the bridge was passing through the remaining two lanes in the meantime, but was moving at a slow pace because of the obstructions. No runs were made when there was any truck in this traffic; only light passenger cars were on the bridge when the data was taken.

The second field test was conducted on October 29 and 30, 1979. The weather was cold and rainy during the tests and the visibility very poor. Preliminary information from the first test indicated that the dynamic data produced more consistent values, so no static truck data was obtained. The lanes were not closed and the normal traffic was allowed to flow on the bridge.

The lane position of the truck was similar to that for run 1 and a constant speed of about 50 mph was maintained over the test span. Since no lanes were closed, the traffic was moving at its normal speed and did not have to slow down. Many runs were made and five of these had almost no traffic on the instrumented and the adjacent span. Therefore the data obtained was due to the test truck alone.

Fig. 2.17 Test truck in lane 1

CHAPTER 3

TEST DATA REDUCTION

The static and the dynamic data collected in the field tests was stored on magnetic tapes by the Vidar system. These tapes were processed on a CDC-Cyber 6600 computer system. Appropriate conversion factors as shown in Appendix B were used to convert the data from voltages to stresses.

3.1 Data Reliability

The static data was recorded for five truck locations, three as described earlier and two with the truck off each end of the bridge. This data was collected twice, once with the truck going forward North to South, then backing up from South to North.

At any one location of the truck, the output of each gage was recorded five times, over a period of about three seconds. The average of the range between the highest and the lowest readings among the five was found to be 0.002 volts, which could be interpreted as normal data scatter. This voltage, corresponds to a stress range of 0.3 ksi, based on the flange gages. If a gage showed a difference of more than 0.002 volts for the two off-bridge truck positions, the reliability of the gage might be questioned. However, this difference was affected by the amount of other traffic on the bridge while the off position readings were being made, so the dynamic data was also used to evaluate the reliability of the data.

When the dynamic data for gages, which are expected to give similar values, were plotted versus time as shown in Fig. 3.1, the gages that are erratic stand out conspicuously. The behavior of gage number 4 is different from that of gages 1, 2 and

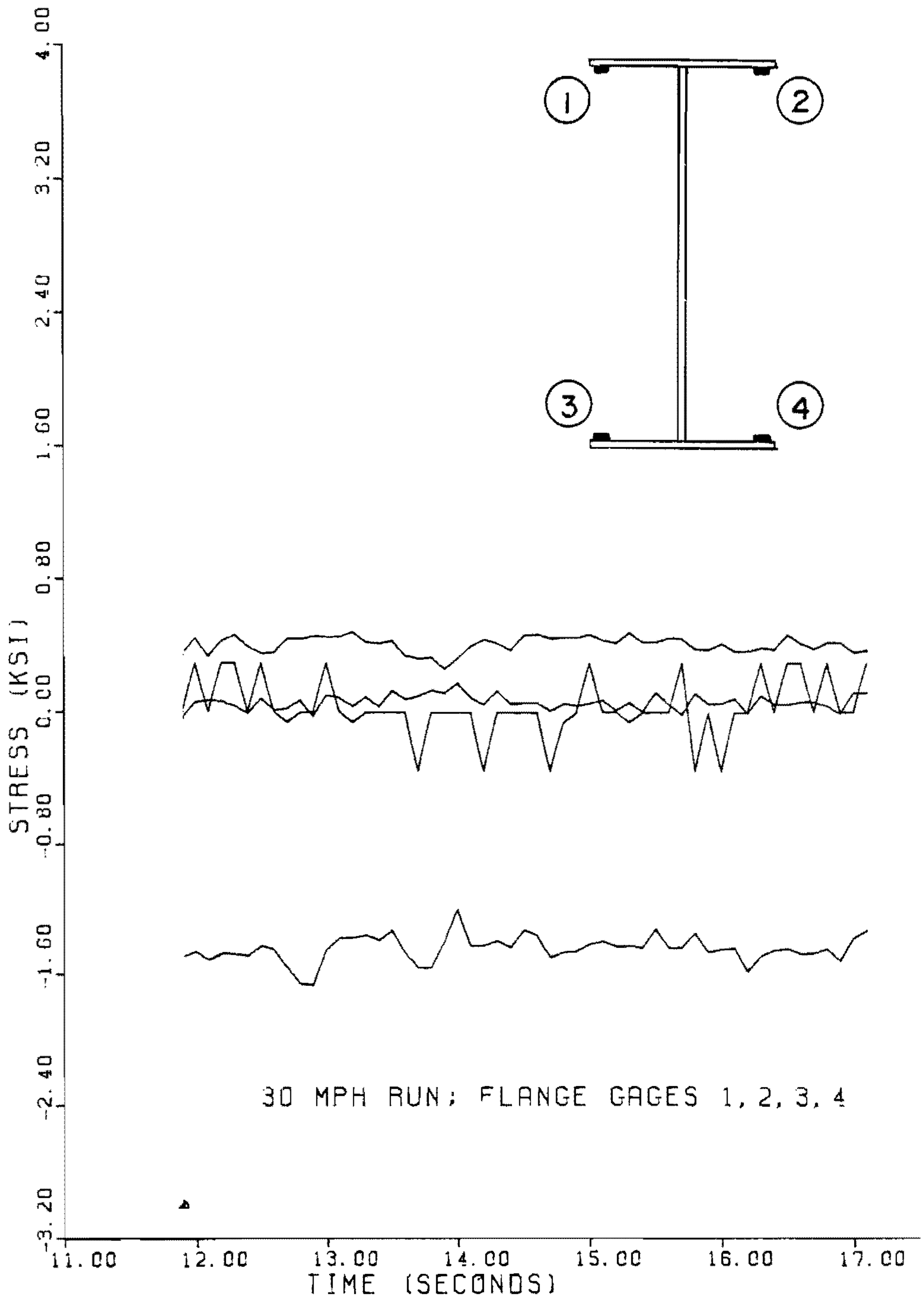

Fig. 3.1 Faulty behavior of gage 4.

3, although all four of them are flange gages. Thus, gage number 4 was discarded. Since the other traffic affects all four gages together, and the data of these four gages was collected over a period of about 0.01 second, a comparison among the four similar pages is valid and unaffected by other traffic. The dynamic data were then used to establish gage reliability.

3.2 Moment Calculations

The strain gages over the cross section were studied in an attempt to establish the location of the neutral axis, the possible composite action between the deck slab and the girder, whether plane sections remain plane, and if the longitudinal stiffener acted as an additional flange, assuming plane sections remain plane during bending.

The difference between the measured and the expected stress over the cross-section was calculated for various truck positions. For example, for the static truck position B, with the truck moving from South to North, the calculations for gages 1-6 are shown below. The positions of these gages are shown in Fig. 3.2. Gage number 4 was found defective by inspection of the dynamic data as shown in Fig. 3.1. Hence it was not used in the calculations. Average of the stresses from gages number 1 and 2 = -1.88 ksi. Stress from gage number 3 = +1.66 ksi. Assuming that plane sections remain plane, the expected stress from gages number 5 and 6 = +0.97 ksi. Average measured stresses from gages number 5 and 6 = +1.12 ksi. The difference between the expected stress and the measured stress is less than 0.3 ksi, the reliability limit. Hence it can be assumed that plane sections do remain plane. This was verified with other truck positions also.

The difference between the top and bottom flange stress is also less than 0.3 ksi, hence the neutral axis of the girder is at

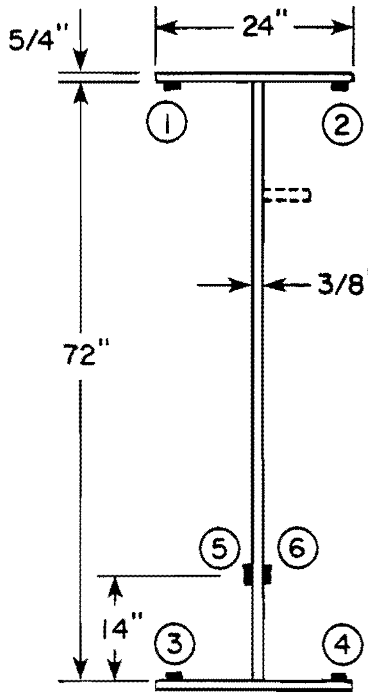

Fig. 3.2 Moment gages

the center. So, the girder is acting alone rather than acting compositely with the slab. The moment in the beam at the gage location shown in Fig. 3.2 can now be easily determined from the formulation $M = f_x I/Y$, where f_x is the average measured flange stress (1.81 ksi for gages 1, 2 and 3), I is the moment of inertia (92155 in^4) and y is the distance from the strain gage to the centroidal axis.

If the stiffener is assumed to be taking part in the flexure of the girder, i.e., acting as a flange, the neutral axis changes position, and the section properties change, as shown in Fig. 3.3. Using the measured strains at the two flanges, and the S_T and S_D as in Fig. 3.3, the calculated moments show a 775 in-K difference whereas the moment corresponding to the stress reliability of 0.3 ksi shows a $0.3 \times 92155/36 = 770$ in-K difference. Since these moments are similar, the difference in the flange strain data can not be interpreted as resulting solely from the longitudinal stiffener acting as a flange. Unfortunately, the measured stress levels are too low compared to the experimental reliability to clearly establish the influence of the longitudinal stiffener.

The comparison presented above was typical so the section will be considered symmetric about the neutral axis for converting strains to moments. Henceforth only the flange gages will be considered and they will be averaged together to find the flange stress at the section.

3.3 Comparison of Static and Dynamic Data

After the dynamic data was converted to stresses, the various reliable flange gage values at a section were averaged together and multiplied by the section modulus, to get the moment.

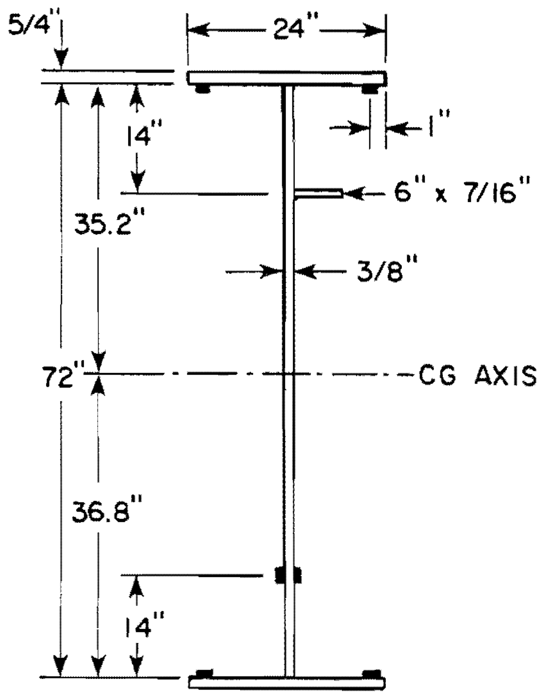

Fig. 3.3 Section with stiffener

$I = 93350 \text{ in}^4$

top = 2652 in^3

bot. = 2537 in^3

This moment was plotted against time. This time axis also represents the truck location along the bridge since the truck speed was reasonably constant. Thus the plot represents the influence line due to the test truck for that particular gaged section. The plot in Fig. 3.4 is an example of such an influence line. The fluctuations in the plot, which have a period of approximately 0.30 sec., are due to the natural vibration of the bridge as shown in Appendix C. These can be eliminated by drawing a mean line through the data.

While taking the static data for any truck location, five scans were made each time, as discussed previously. Hence, five moment values can be determined for each truck location. The difference in the five static data values can be attributed to bridge vibrations and variation in the other traffic. To get the five measured values from the static data, the average of the five off bridge position scans for each gage was subtracted from each one of the five scans for the corresponding gage. The various flange stresses were averaged together and multiplied with the section modulus multiplier. This process has been explained with an example in Appendix D. The five moment values due to the static truck will be compared with the dynamic response later.

The dynamic data for the medium speed runs, i.e. at approximately 30-35 mph, was scanned at an interval of 0.05 secs. The electronic timing device attached to the Vidar system in its Mode operation, as explained in Chapter 2, was set at this value. In Mode 2 operation the Vidar produces incorrect data every other scan, due to a problem with the tape buffer. So the actual interval of scanning was 0.1 secs.

The particular scan corresponding to the truck positioned at the support location can be identified visually from the dynamic data plot. As seen in Fig. 3.4, the truck passes over the

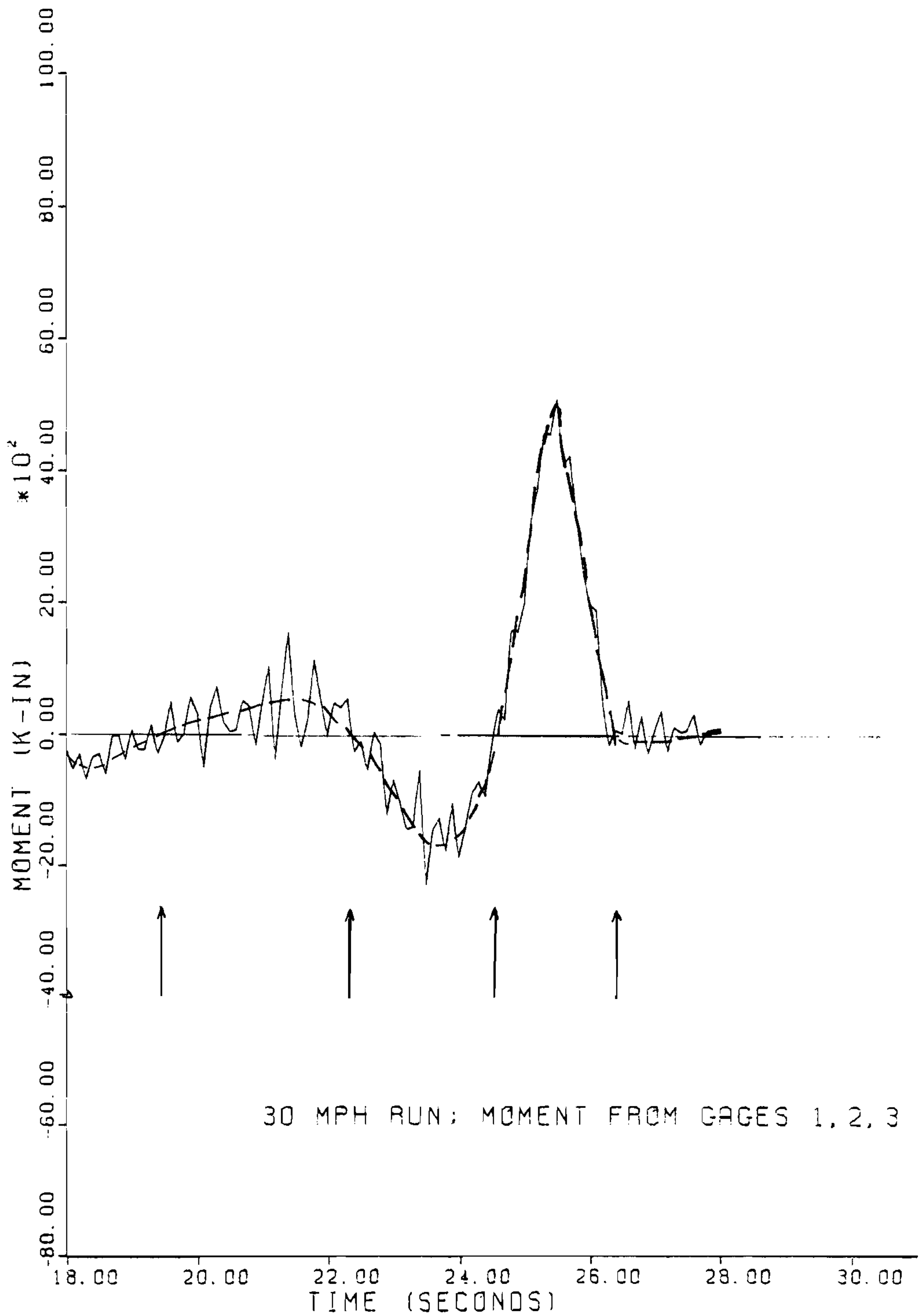

Fig. 3.4 Dynamic moment data

supports at scans number 224, 246.5 and 264 approximately, i.e., at 22.4, 24.65 and 26.4 seconds. Knowing the scan rate and the distance between the supports, the velocity of the truck can be determined. The scans corresponding to the static locations of the truck can also be determined. Referring back to Fig. 2.15, scan 264 (26.4 secs) corresponds to the end support and scan 246.5 (24.65 secs) to the first interior support. Hence position C corresponds to scan 259 (25.9 secs) and position B to scan 256 (25.6 secs). The resultant of the rear wheels of the truck was assumed to be at these positions. No differentiation could be made in the front and wheel effects due to limitations in clarity of data. However, in a relative study of truck positions, this is insignificant.

The static moment values for truck locations B and C were compared to the dynamic response at scan numbers 256 and 259 respectively. The static data was plotted on the dynamic curves and one is shown in Fig. 3.5. This is a plot of the reaction the hanger and hence the other traffic on the bridge has a effect on it. As can be seen, there is a lot of scatter in the static data. Some of the points match up well but the rest are far off. This probably occurs due to the natural vibration of the bridge. Since a reliable mean cannot be found as in the dynamic data, the static data is not trustworthy. Consequently only the dynamic data will be compared with the theoretical analysis.

3.4 Distribution to Other Girder

Having measured the moment in both the girders separately, the distribution of the moment among the two girders can be calculated. Since the test truck was positioned just over one of the girders, the distribution of the load between the two girders is due to the connecting slab and crossbeams. The ratio of the moment

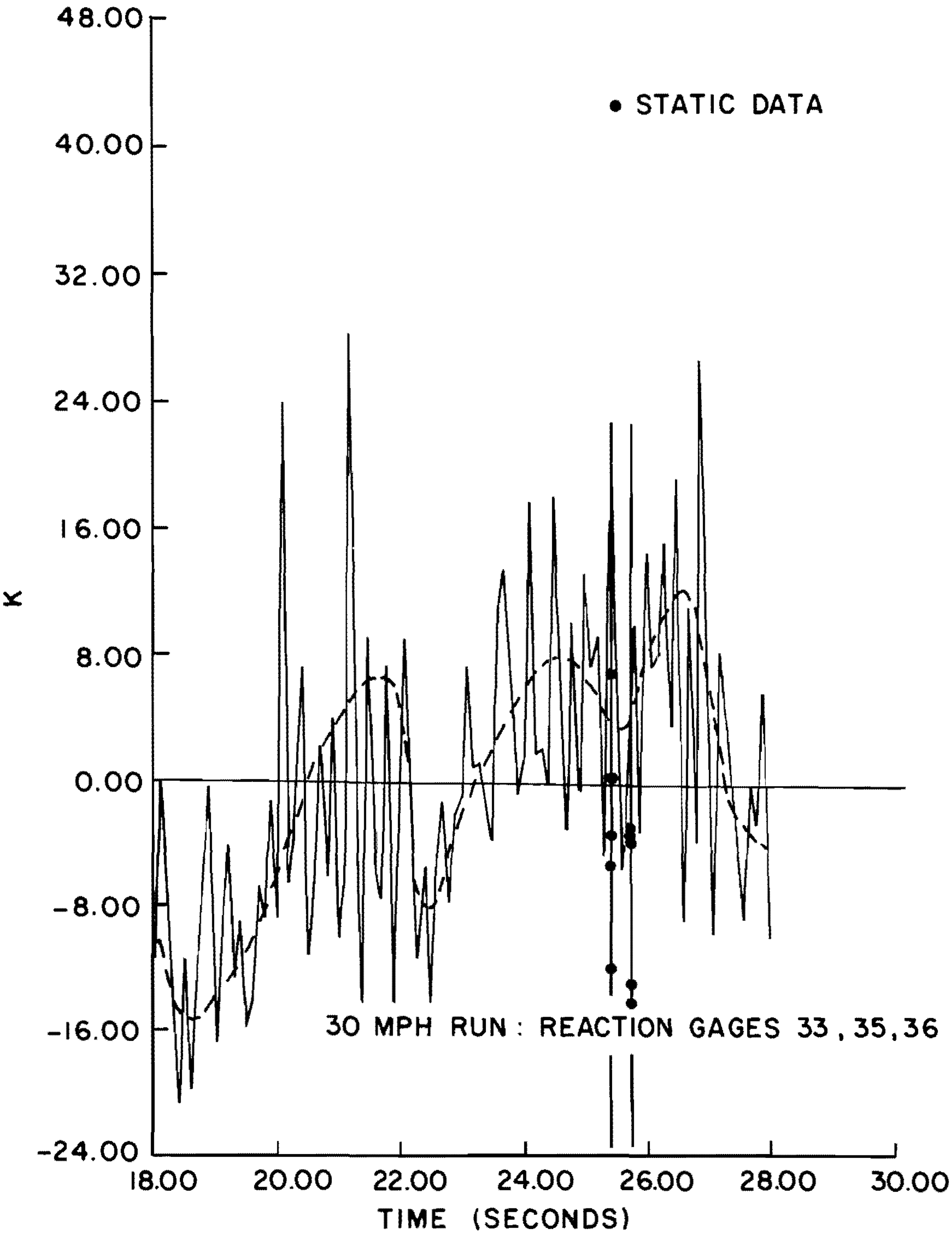

Fig. 3.5 Comparison of static and dynamic data

in the other girder to the total moment is shown in Table 3.1. The distribution at gage location I is about 26%, whereas at gage location II it is about 15%.

An approximate theoretical analysis was done, using the SAP4 program, to find the moment distribution among the girders. Only the grid system of girders and cross-beams was considered. The results were compared to the actual distribution in Table 3.1. The analysis predicts a higher distribution to the other girder than found in tests. This may be due to the interaction of the slab with the grid.

According to AASHO specifications for Highway Bridges [5], the live load bending moment for outside roadway beams shall be determined by applying to the beam the reaction of the wheel load obtained by assuming the flooring to act as a simple span between beams. Even when considering the beams to be interior beams, the same is valid. The test truck being stationed on top of one of the girders, all the load is then to be assumed to be carried by that girder.

TABLE 3.1 DISTRIBUTION OF MOMENTS TO OTHER GIRDER

Truck Location	Gaged Sections	Distribution Actual 5 mph	Distribution Actual 35 mph	Distri-bution Analytical
28' from south end support	Section I	0.25	0.29	0.52
	Section II	0.14	0.21	0.26
40' from south end support	Section I	0.26	0.27	0.22
	Section II	0.13	0.15	0.30
42' from second last support	Section I	0.31	0.19	
	Section II	0.07	0.16	

CHAPTER 4

TEST DATA EVALUATION

4.1 Analysis of the Bridge

The bridge under study is a five span structure, with two main steel girders, 72" deep. It supports 48" deep cross beams at a spacing of 18' in the first span and 19'7" in the other spans. A 10-1/2" thick continuous post-tensioned concrete slab rests on the cross beams. The slab is connected to the cross beams by loose anchor-bolts, thus preventing any lateral movement between the beam and the slab.

The structure was modelled as a one-story frame, as shown in Fig. 4.1. The top members, numbered 25 to 47, represent the slab; hence they are assigned the Moment of Inertia, Modulus of Elasticity and a cross-sectional area of the slab. Similarly, the bottom members, numbered 48 to 80, represent the continuous girder. The vertical members represent the cross beams. In the actual structure only the lateral movement of the slab with respect to the cross-beams is restricted, rotational freedom is provided. Hence the axial members of the model, numbered 1 to 24, are assigned a very small moment of inertia, but a large cross-sectional area.

The truck is assumed to be loading one longitudinal girder only. Hence the members numbered 48 to 80 represent only one girder. Members 25 to 47 represent half the slab only, since the other half of the slab is supported by the other girder.

The moment in the girder depends on the moment carried by the slab, as shown in Fig. 4.3. For a certain loading, the reaction at support A is fixed, and hence, the sum of the girder and slab moment at a cross-section is also fixed by static equilibrium.

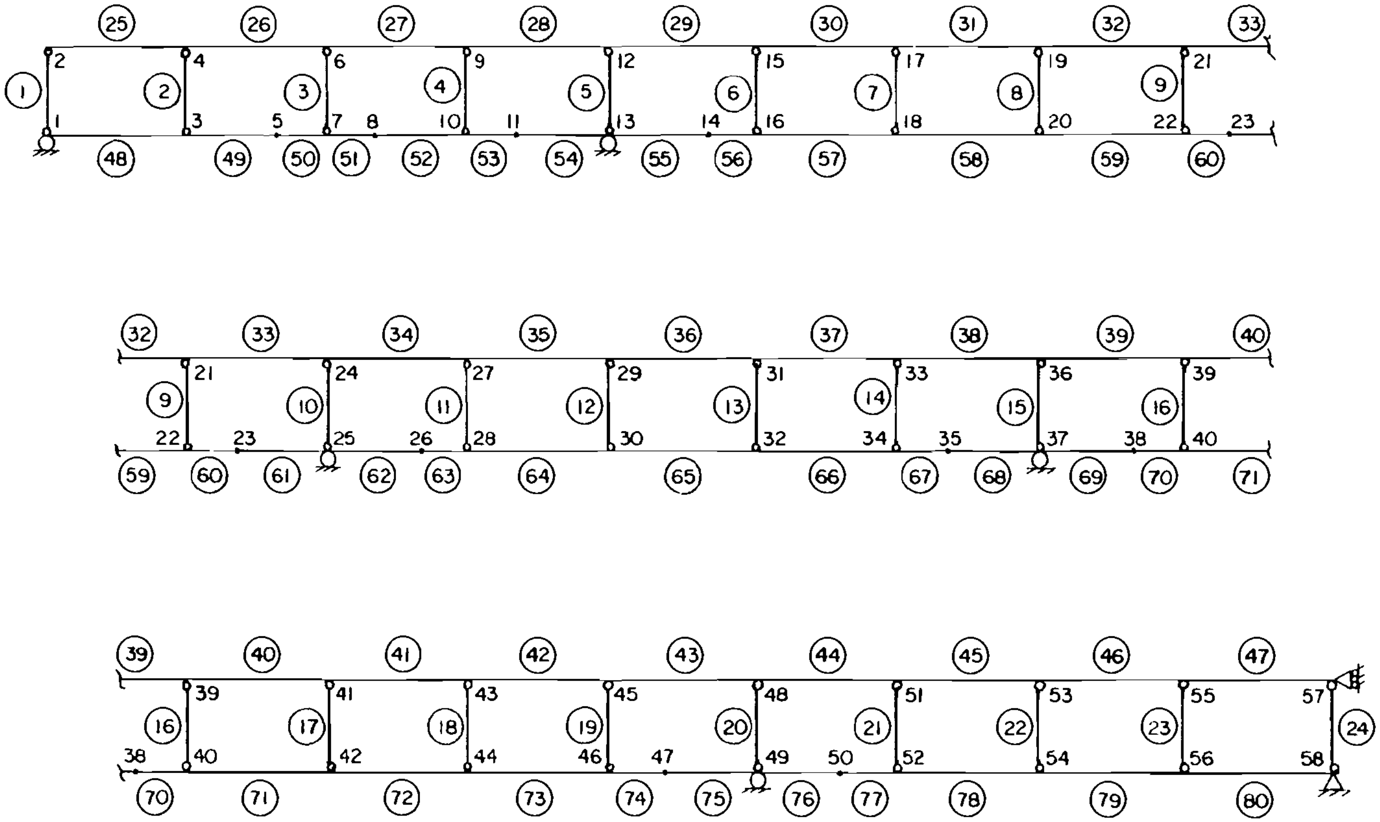

Fig. 4.1 Frame model of the bridge

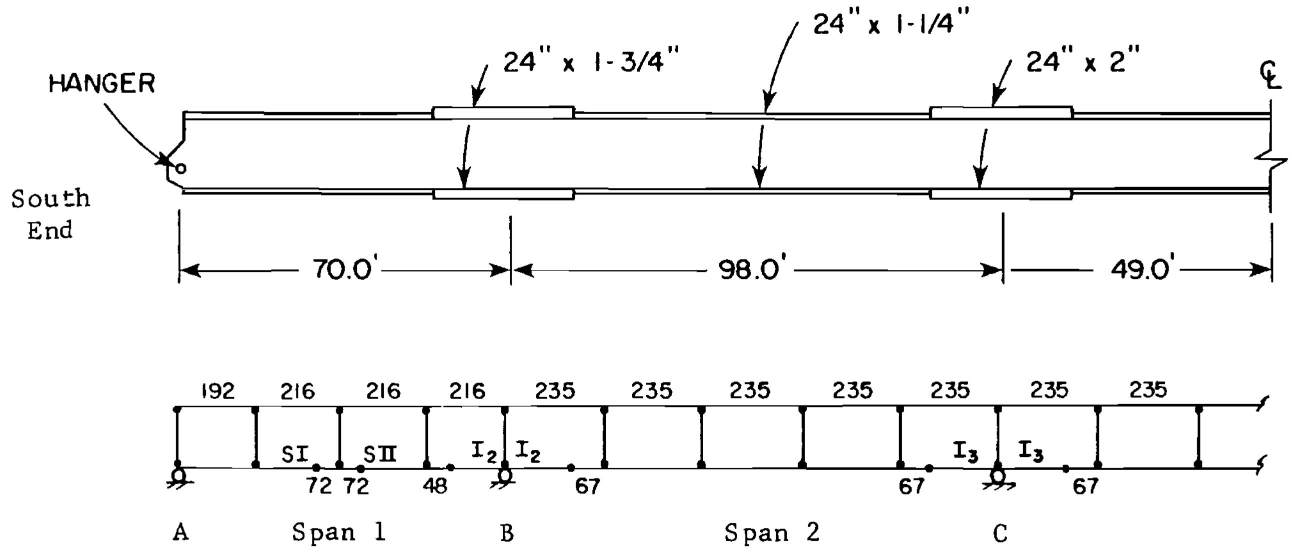

Fig. 4.2 Girder dimensions

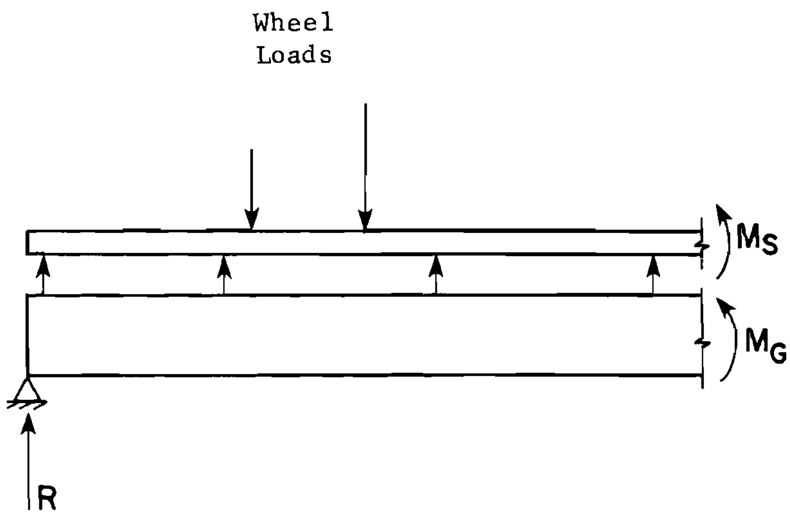

Fig. 4.3 Reactions due to the truck load

So, as the moment carried by the slab reduces near the slab supports, the moment in the girder increases.

The girder flanges increase in thickness near the supports, thus changing the sectional properties, especially the moment of inertia. These changes have been incorporated into the model, as shown in Fig. 4.2. The amount of inertia I, the modulus of elasticity E, and the cross sectional area A that have been used are shown below.

Slab:	Dimensions = 10-1/2" × 414"
	$I = 40{,}000\ in^4$
	$E = 4000$ ksi
	$A = 4347\ in^2$
Girder:	$I_1 = 92155\ in^4$
	$I_2 = 125905\ in^4$
	$I_3 = 143120\ in^4$
	$E = 29{,}000$ ksi
	$A = 100\ in^2$
Cross-beams	$I = 1\ in^4$
	$E = 29{,}000$ ksi
	$A = 5000\ in^2$

The model was analyzed using a computer program for the solution of plane-rectilinear frames. The program has been written by Dr. C. P. Johnson and is available on the University of Texas at Austin computer system. The program computes displacements and rotations at the nodes, and forces and moments in the members. It also computes the joint equilibrium forces at the nodes.

Analysis was done for three positions of the truck on the bridge moving North to South. These three positions were, 1) the rear axle of the truck, 28 feet from south end support, i.e., almost over the gaged section I, 2) the rear axle of the truck, 40 feet from south end support, i.e., almost over the gaged section II, and 3) the rear wheel of the truck, 42 feet from support B.

Two positions were chosen in the first span to ensure that the results are indpendent of the position of the truck. These positions are also near the center of the span, where the moment values are the largest.

The moment at node 5 at the end of member 49 and the moment at node 8 at the end of member 51 were noted. These correspond to gage location I and II respectively. The reaction at the first support was found from the joint equilibrium forces at node 1, as shown in Fig. 4.2. For the first truck position, i.e. the rear axle 28 feet from support A, as shown in Fig. 4.4, the moment at node 5 of member 49 = 6421.83 k-ins, the moment at node 8 of member 51 = 4893.74 k-ins, joint equilibrium force at node 1 in y direction = 31.94 kips. Similarly the moments and the reaction were read for the second and third positions, and the results are summarized in Table 4.1.

4.2 Dynamic Test Data

Data corresponding to the three truck locations chosen in Sec 4.1 was determined from the mean moment plot, as shown in Appendix E. The reactions were also similarly determined. The cross-beams share the load of the truck on the slab. So, the loading on the girder depends on the distribution of the load among the floor beams. This has already been determined in the theoretical analysis. Both the girders share the load, reacting together. The theoretical analysis however is two-dimensional. So, to compare the test data with the analytical solution, measured

Member No.	Node No.	Axial Load	Shear	Moment
47	55	.04	-.01	-1.25
	57	-.04	.01	-.02
	MID-SPAN MOMENT =		.617	
48	1	-.09	30.57	2.18
	3	.09	-30.57	5866.36
	MID-SPAN MOMENT =		2932.092	
49	3	-.15	3.87	-5864.76
	5	.15	-3.87	6421.83
	MID-SPAN MOMENT =		6143.295	
50	5	-.15	3.87	-6421.83
	7	.15	-3.87	6700.37
	MID-SPAN MOMENT =		6561.104	
51	7	-.12	-25.10	-6700.97
	8	.12	25.10	4893.74
	MID-SPAN MOMENT =		5797.357	
52	8	-.12	-25.10	-4893.74
	10	.12	25.10	1279.29
	MID-SPAN MOMENT =		3086.517	
53	10	-.07	-20.68	-1280.62
	11	.07	20.68	288.05
	MID-SPAN MOMENT =		784.335	
54	11	-.07	-20.68	-288.05
	13	.07	20.68	-3185.92
	MID-SPAN MOMENT =		-1448.934	

Fig. 4.4 Typical moment output for first truck location

moment values from both the girders were simply added together. The measured and the expected variables are compared in Table 4.1. For the 30 mph run, the measured values are within 10-15% of the analytically predicted values. The error is greater whenever the slab moments are small, i.e., the inflexion point is close by. So a slight mistake in the determination of the scans corresponding to the truck positions would change the slab moments tremendously, thus changing the girder moments also.

For the 5 mph run, the truck stays on the bridge for a longer time, so other traffic affects the data. For that reason also, the reactions are very high. For the 50 mph run, the difference between the test results and the analytical solution is 15 to 20%. The data follows the pattern of the predicted moment values.

4.3 Truck Location Reliability

The static data has the advantage that the truck location is exactly known when the data is recorded. So the measured amount can be compared with the analytically predicted moment for the same location. However, the problem of girder vibration remains.

In the dynamic data, the bridge vibrations can be eliminated, but the truck location is not exactly known, and can at best be approximated only. The location of the supports is decided by visually inspecting the influence line and is not exact.

For the 30 mph data, the speed may not be exactly 30 mph all the time. The truck speed could have been 10% off either way, which corresponds to one scan interval (0.1 seconds). Initially, scans 257, 254 and 237 were chosen as the scans that correspond to the truck locations (Sec 4.1). However, scans 258, 255 and 238 may be the correct scan, as shown in Table 4.2. Using the new positions

TABLE 4.1. COMPARISON OF MEASURED AND PREDICTED VALUES OF VARIABLES

Truck Location	Variable	Analytically Predicted Value	Slab Moments	Measured Value	Measured/ Analytical	Measured Value	Measured/ Analytical	Measured Value	Measured/ Analytical
28' from south end support	Moment at Section I (k-in)	6422	1479	5215	0.81	5425	0.84	5101	0.80
	Moment at Section II (k-in)	4894	-99	4550	0.93	3620	0.74	4025	0.82
	Reaction from Hanger (k)	31.9	--	37.9	1.19	29.5	0.92	--	--
40' from south end support	Moment at Section I (k-in)	6445	146	5432	0.84	6800	1.06	4973	0.77
	Moment at Section II (k-in)	6196	1519	5890	0.95	5670	0.92	5130	0.83
	Reaction from Hanger (k)	21.6	--	32.9	1.52	19.7	0.91	--	--
42' from second last support	Moment at Section I (k-in)	-2346	-143	-3215	1.37	-1920	0.82	-1873	0.80
	Moment at Section II (k-in)	-3353	-200	-2160	0.64	-2900	0.87	-2985	0.89
	Reaction from Hanger (k)	-7.42	--	+15.0	0.99	-1.0	--	--	--

TABLE 4.2 TRUCK ON NEW POSITIONS 30 MPH

Truck Location	Variable	Old Position Measured Value	New Position Measured Value	Analytically Predicted Value	Ratio: Measured/ Analytical
28' from south end support	Moment at Section I (k-in)	5425	4776	6422	0.74
	Moment at Section II (k-in)	3620	2705	4894	0.55
	Reaction from hanger (k)	29.5	32.4	31.9	1.02
40' from south end support	Moment at Section I (k-in)	6800	6953	6445	1.08
	Moment at Section II (k-in)	5670	5245	6196	0.85
	Reaction from hanger (k)	19.7	25.9	21.6	1.20
42' from second last support	Moment at Section I (k-in)	-1920	-1954	-2346	0.83
	Moment at Section II (k-in)	-2900	-2883	-3353	0.86
	Reaction from hanger (k)	-1.00			

the ratio of the measured value to the analytically predicted value changes by approximately 10%. This is a high value considering that the readings have been changed by only one scan. This indicates that scans should be taken at a faster rate than 0.1 secs. Also, any mechanism used to locate the position of the truck on the bridge would need to have a response time of at least less than a scan interval.

CHAPTER 5

SUMMARY AND CONCLUSIONS

The structural behavior of a twin girder steel bridge system was studied in the field. Strain gages were placed on an appropriate section of a chosen span. A 52 kip truck was used to load the bridge. It was placed at certain locations on the bridge for static data. Dynamic runs at three different speeds of 5 mph, 30 mph and 50 mph were also made. The bridge was also modelled as a frame structure, and analyzed theoretically.

On comparing the measured data with the theoretical values, it is found that results are close to the experimental error range of 10%. Hence, the model that has been used to represent the structure is fairly accurate.

The 30 mph run compares better with the theoretical values than the 5 mph run. Faster runs are better because the effect of the other traffic is less.

In the dynamic runs a better estimate of the truck location on the bridge is desirable. Knowing exactly where the truck was when a particular scan was made would improve the reliability of the data.

However, the problem of truck location can be completely solved by placing the truck at a fixed location and taking the data continuously for a second or two. Our static data was not used because the data was taken instantaneously and so the effect of bridge vibrations on the data could not be removed.

The maximum stress range was found to be 3.1 ksi in the main girder, when the test truck passes over it. This is acceptable since the allowable stress range for a category E′, the worst fatigue category, is 5.8 ksi upto 2,000,000 cycles and 2.6 ksi for over 20,000,000 cycles (Fig. 1.2). The test truck used was very heavy and with a small wheel base. Most probably this is one of the heaviest loads the bridge is going to experience. So, the problem is not so severe and immediate unless some of the bridge details are worse than E′.

An approximate theoretical analysis of the bridge as a steel grid structure was done to predict the moment distribution between the twin girders. The analytical model which neglected the slab did not give satisfactory results in predicting the load transfer between the two girders. An analysis should be performed incorporating the slab in the model.

R E F E R E N C E S

1. Fisher, J. W., Research Results Digest, Fritz Engineering Laboratory, Lehigh University, Bethlehem, Pa., Digest 59, March 1974.

2. Fisher, J. W., Bridge Fatigue Guide, Design and Details, American Institute of Steel Construction, Chicago, 1977.

3. AASHTO Subcommittee on Bridges and Structures, Standard Specifications for Highway Bridges, American Association of State Highway and Transportation Officials, Twelfth Edition, Washington, D. C., 1977.

4. Covarrubias, J. S., Frequent Overloads, Engineering News-Record, Vol 196, No. 23, Reader Comment, June 3, 1976, p 5.

5. Fisher, J. W., A. W. Pense, and R. Roberts, Evaluation of Fracture of Lafayette Street Bridge, Journal of the Structural Division, ASCE, Vol 103, No. ST7, Proc. Paper 13059, July 1977, pp 39-57.

A P P E N D I X   A

CANTILEVER-TYPE DEFLECTION GAGES

APPENDIX A

CANTILEVER-TYPE DEFLECTION GAGES

The deflection gage consists of a triangular, elastic, aluminum plate stiffened at the base. The base is clamped to the flange of the girder, where the deflection is to be measured. The gage then protrudes from the flange like a cantilever, as shown in Fig. A1. A piano wire is attached to the apex of the triangle and suspended so that it reaches the ground. Weights, resting on the ground, are attached to the other end of the wire, to keep it in tension and bend the cantilever.

The gage can be represented by a cantilever of varying moment of inertia and with a spring at the end, as shown in Fig. A2. At any distance y from the spring-loaded end, the moment of inertia can be represented by $I_y = I(y/\ell + c)$.

where $I = b_1 d^3/12$ and $c = a/b_1$

The structure can be divided into two determinate systems, as shown in Fig. A3.

$$M = 1 \times y = y$$

$$\therefore \delta_p = \int_o^\ell y^2/E(I(y/\ell + c))dx$$

$$= \frac{1}{EI}\int_o^\ell y^2/(\frac{y}{\ell} + c)dx$$

$$= \frac{1}{EI}[\ (1 + c)\ell^3(0.5 - 1.5c) + c^2\ell^3\ell n(1 + c) + c^2\ell^3(1.5 - \ell nc)\ ]$$

$$= \frac{1}{EI}f(c,\ell)$$

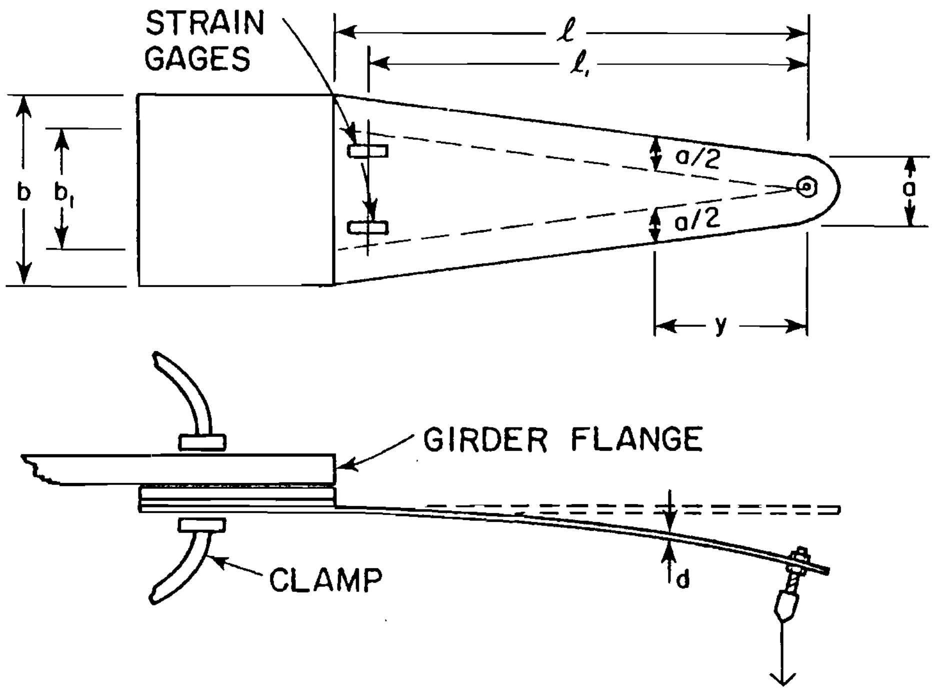

Fig. A1 Cantilever-type deflection gage

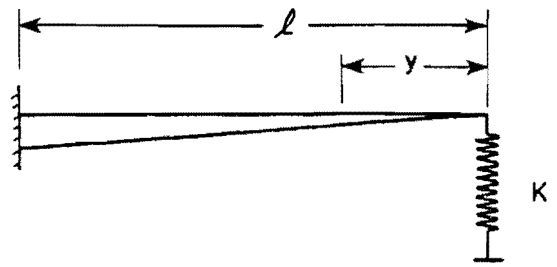

Fig. A2 Analytical model of deflection gage

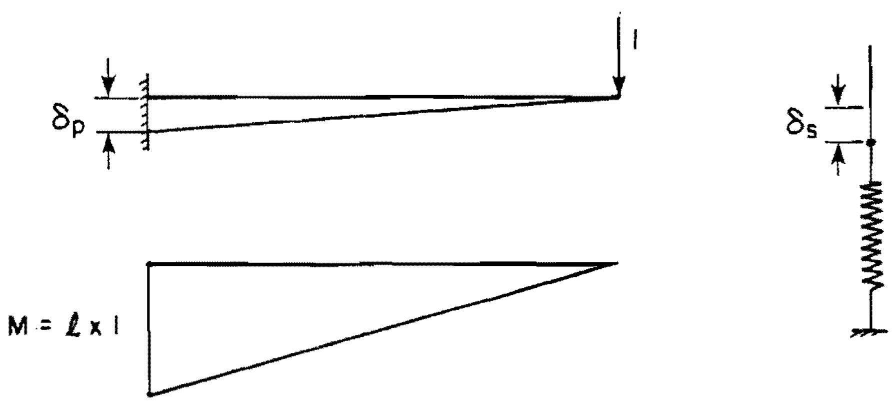

Fig. A3 Determinate systems of the structure

$\delta s = 1/k$ where k is the spring constant.

$\therefore X\delta_p - X\delta_s = \delta$ initial, where X = tension in the wire,

$\therefore X\left(\frac{f(c,\ell)}{EI} - \frac{1}{k}\right) = \delta$ initial

$\therefore X \,\alpha\, \delta$initial

Drawing the moment diagram for the cantilever, as shown in Fig. A3,

$M = X \times \ell_1$

$M \,\alpha\, \delta$initial

ϵ measured α δinitial

Since the measured strain is directly proportional to the initial deformation, the ratio of the strain measurements to the bridge deflection is independent of the initial tension in the wire.

$$X\left(\frac{f(c,\ell)}{EI} - \frac{1}{k}\right) = \delta$$

$$\frac{f(c,\ell)}{EI} = \frac{1}{EI}\left[\,(1 + c)\ell^3(0.5 - 1.5c) + c^2\ell^3\ell n(1 + c) + c^2\ell^3(1.5 - \ell nc)\,\right]$$

where $c = a/b_1 = 1/3.375 = 0.296$

$\ell = 12$ in

Modulus of Elasticity of Aluminum = 10,000 ksi

$\therefore \frac{f(c,\ell)}{EI} = 104.9$ in/kip

$$\frac{1}{k} = \frac{L}{AE}$$

where L = length of piano wire

A = cross-sectional area of wire = $\frac{\pi}{4} \times 0.0175^2$

E = Modulus of elasticity of steel = 29,000 ksi

$$\therefore \frac{1}{k} = \frac{L}{6.975} \text{ in/kip}$$

Hence $\mathbf{X}(104.9 - L/6.975) = \delta$ (i)

From the moment diagram in Fig. A3,

$$\mathbf{X} = \frac{M}{\ell_1} = \frac{fcI(\ell_1/\ell + c)}{\ell_1 d/2}$$

where fc = stress in the extreme fiber of the cantilever at a distance of ℓ_1 from the wire.

$$= \frac{\epsilon EI(\ell_1/\ell + c)}{\ell_1 d/2}$$

$$= (7.328 + 26.048/\ell_1)\epsilon \qquad \text{(ii)}$$

From (i) and (ii),

$$\delta/\epsilon = (7.328 + 26.048/\ell_1)(104.9 - L/6.975)$$

The relation between the deflection and measured strain was experimentally determined in the laboratory also, using the wire lengths L used in the field. The results were found to be very close to the theoretical values. The theoretical values were then used in calculations.

A P P E N D I X   B

STRAIN GAGE DATA REDUCTION

A P P E N D I X B

STRAIN GAGE DATA REDUCTION

Two types of input were used with the high speed Vidar,

(1) Strain gage with 1 external completion resistor and 2 resistors present in the signal amplification circuit, i.e. 1/4 bridge [Fig. B1(a)]

(2) Full bridge input with no external completion resistors, used for deflection gages [Fig. B1(b)].

A DC power source was used to supply a bridge voltage of approximately 2 volts. This voltage was varied by adjusting the output of the power supply.

The output signal from the strain gage circuit was given a gain of 400, i.e., it was amplified 400 times, so as to obtain results of greater accuracy over a larger voltage range. Computer software was developed to convert the binary coded data on the magnetic tape to voltages. Strain may then be calculated, using the following relationship,

$$\epsilon = 2.0/\text{bridge voltage} \times \text{channel voltage}/400$$

This relationship assumes the gage factor is equal to 2.0. The actual values were within 1% of 2. The bridge voltage was recorded in channel 0, each time a scan was made. If the bridge voltage is 2.0, the channel voltage divided by the gain is identically equal to the strain. This strain, when multiplied by the modulus of elasticity = 29,000 ksi, gives the stress.

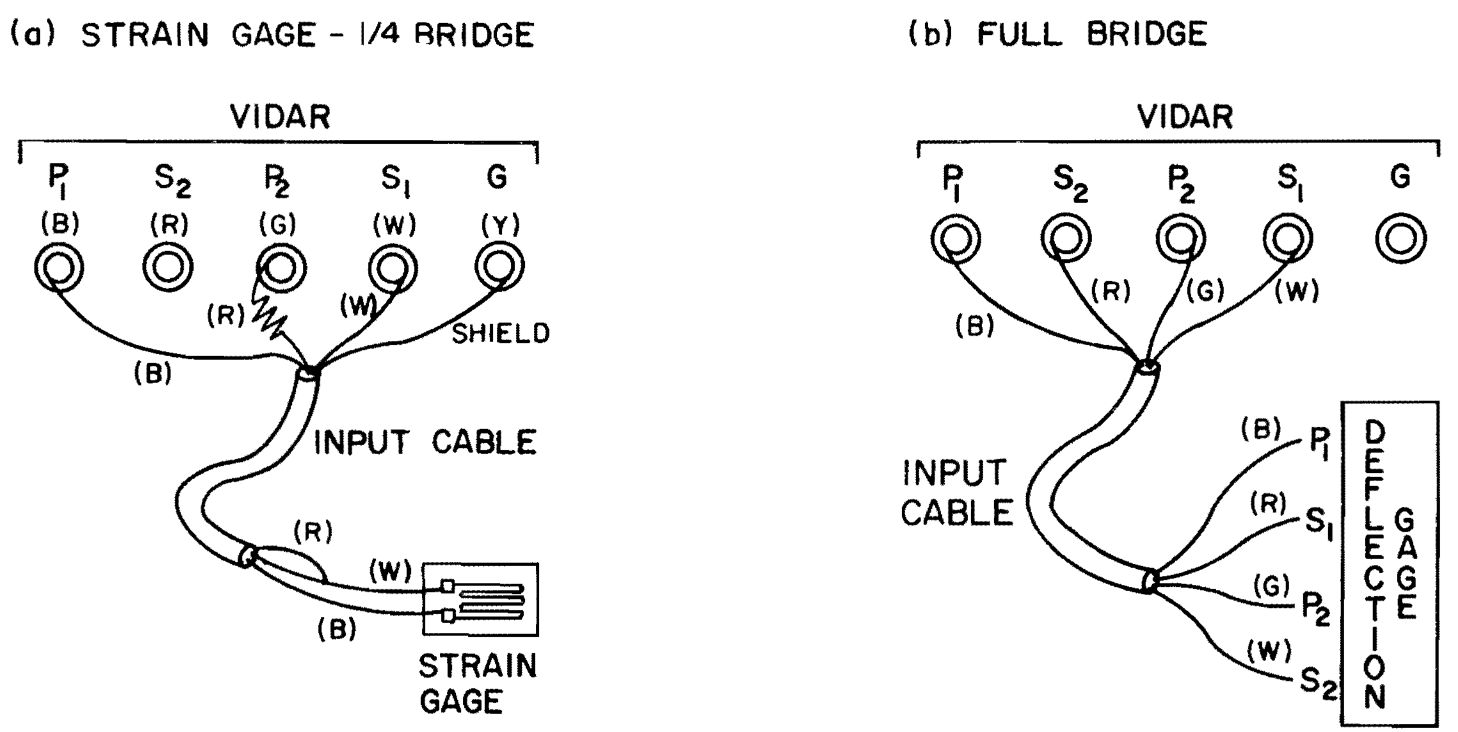

—WW—	120Ω COMPLETION RESISTOR
P_1 :	(+) BRIDGE VOLTAGE
P_2 :	(−) BRIDGE VOLTAGE GROUND
S_1 :	SIGNAL OUTPUT
S_2:	SIGNAL OUTPUT

COLOR CODE

(B) BLACK
(R) RED
(G) GREEN
(W) WHITE (CLEAR)
(Y) YELLOW

Fig. B1 Input cable hook-up. Plug connectors located on the signal input panel are represented by concentric circles.

A P P E N D I X   C

BRIDGE VIBRATIONS

APPENDIX C

BRIDGE VIBRATIONS

A structure vibrates at its natural frequency when it is disturbed. An estimate of the natural period of vibration can be made by analyzing an idealized representation of the actual structure. The first span of the bridge was idealized as a propped cantilever as shown in Fig. C1. The second support from the left acts almost like a fixed end because of the four continuous spans after it.

Hence, T, the natural period of vibration = $0.0722 \left(\frac{WL^4}{EI}\right)^{1/2}$

EI for the two steel girders = $30 \times 10^6 \times 92155 \times 2 = 5.529 \times 10^{12}$ lb-in^2

EI for the concrete deck = $57000\sqrt{4000} \times 40517 \times 2 = 2.921 \times 10^{11}$ lb-in^2

$\therefore$ EI for the bridge = 5.821×10^{12} lb-in^2

weight of slab = 131 lbs/sq ft = 9170 lbs/ft width of slab

weight of girder = 3.4 lbs/in^2/ft = 296 lbs/ft length of girder

$\therefore$ weight of bridge = [9170 + (296 x 2)]/12 = 813.5 lbs/in. length

$$\therefore T = 0.0722\sqrt{\frac{813.5 \times (70 \times 12)^4}{5.821 \times 10^{12} \times 32.2}} = 0.36 \text{ secs}$$

As can be seen from Fig. C2, there are about 5.5 fluctuations between the time 20.0 and 22.0 seconds. Therefore, the time period of the fluctuation is 2.0/5.5 = 0.36 secs.

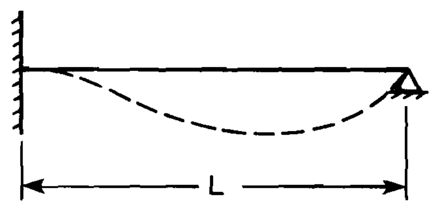

Fig. C1 Propped Cantilever

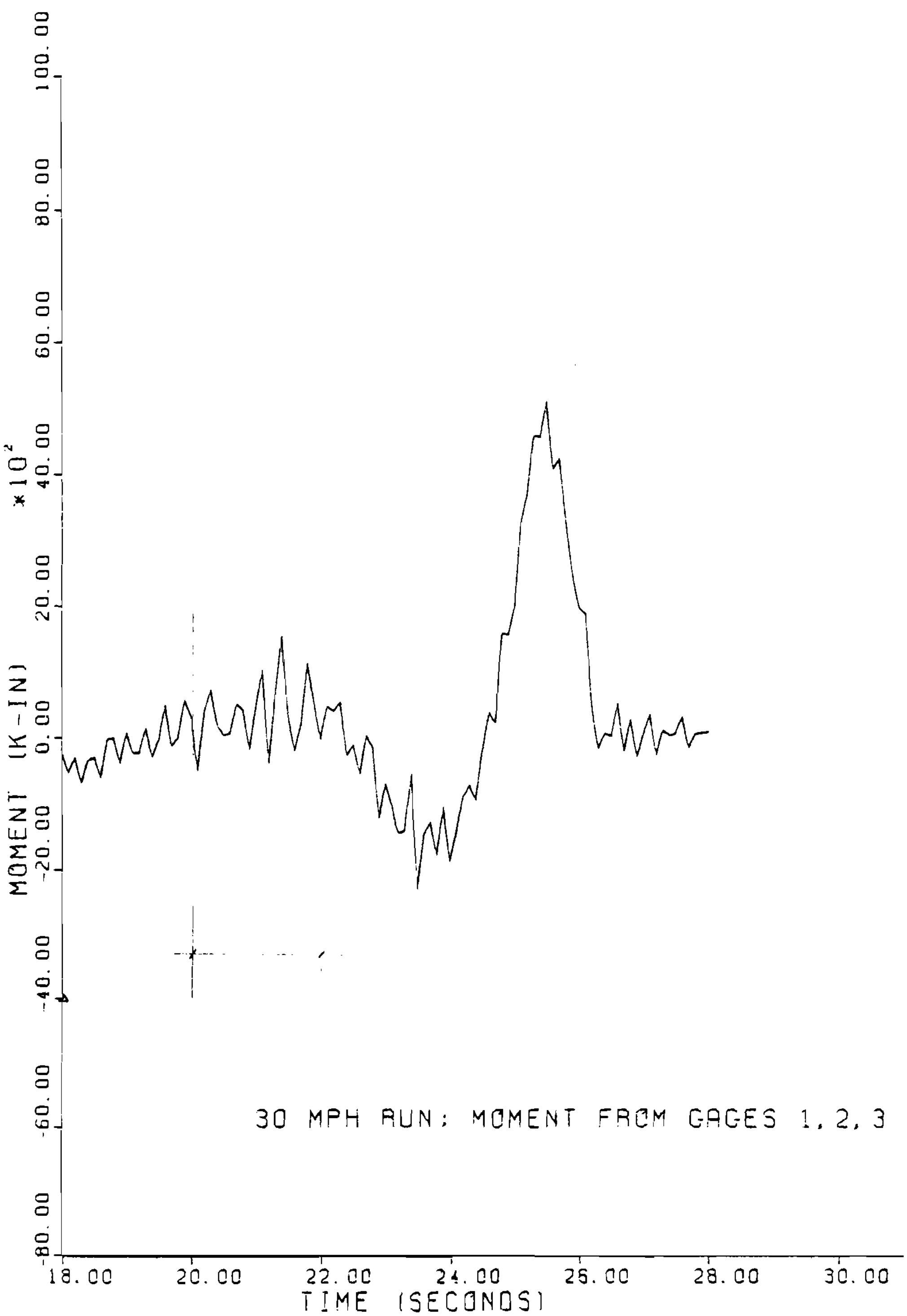

Fig. C.2 Time period of fluctuation = 0.36 secs

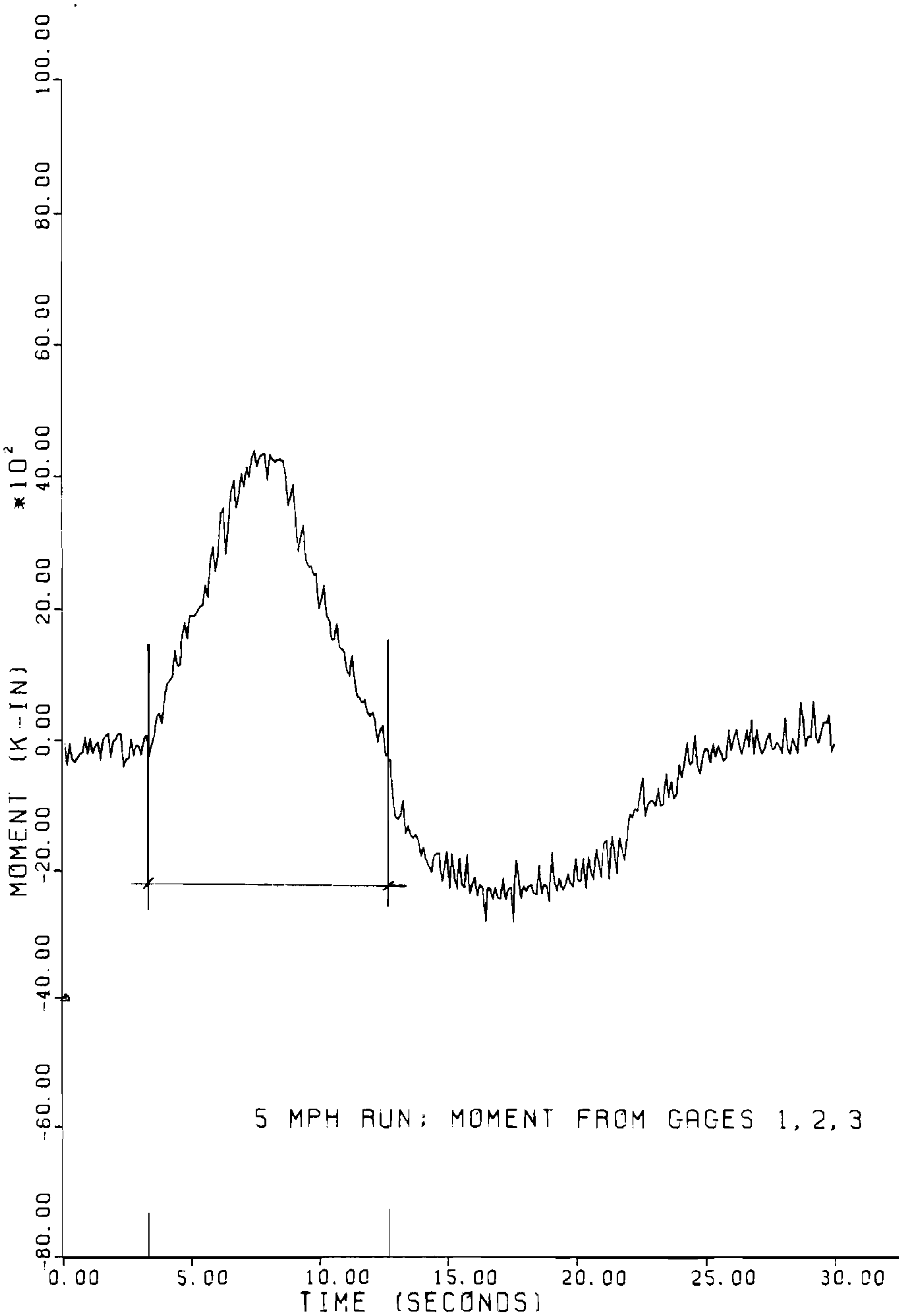

Fig. C.3 Time period of fluctuation = 0.31 secs

For the 5 mph run, the scans corresponding to the first two supports are 33 and 126. Hence, 93 scans were made on the first span. The scanning rate is 0.1 secs. So, the truck was on the first span for 9.3 secs. As can be seen from Fig. C3, there are about 30 fluctuations between the time 3.3 and 12.6 seconds. Therefore, the time period of the fluctuation is 9.3/30 = 0.31 secs.

These time periods of 0.36 and 0.31 secs for the fluctuation in the recorded data are very close to the approximate time period of natural vibration of the bridge, i.e. 0.36 secs. So, it can be deduced that the fluctuations are due to the natural vibration of the bridge.

A P P E N D I X   D

STATIC DATA REDUCTION

APPENDIX D

STATIC DATA REDUCTION

The static data was collected at five truck locations, three as described earlier in Chapter 2, and two with the truck off each end of the bridge. While taking the static data at any truck location, five scans were made each time. Hence, five readings are available corresponding to each truck location, so five moment values can be determined for each truck location.

The data taken at position A of the truck, i.e. rear axle 25 feet from the south end support, is shown in Fig. D1. All the five scans are present, with data recorded in 40 channels for each scan. The data is for the first static run, i.e. truck moving from north to south.

The data from each set of five scans was averaged together. The average data for the first off position of the truck, i.e. north end off position, is shown in Fig. D2. The lowest and highest scan readings corresponding to each gage is also shown. This summary was initially used to reject gages that showed a high variation in their five scans. The difference in the scans can be attributed to bridge vibrations and variation in the other traffic.

To get the five measured values from the static data, each one of the five scans for a particular gage, as shown in Fig. D1, was subtracted from the average of the five off position scans for the corresponding gage, as shown in Fig. D2.

HS VIDAR

1	1.9863290	2	0.0603638	3	4.8007820	4	0.1796876	5	0.2091065
6	0.2294923	7	-0.1237794	8	0.2207032	9	0.3747559	10	0.2220460
11	0.0062103	12	0.2043458	13	0.1262208	14	0.0025024	15	0.1224366
16	0.0614319	17	0.0369873	18	-0.0008087	19	4.5468760	20	0.0936890
21	0.0047913	22	0.0029907	23	0.6035157	24	0.3747559	25	0.0039978
26	0.1728516	27	0.0776367	28	0.0089264	29	0.2541505	30	0.2507325
31	0.0811157	32	0.3217774	33	0.4821778	34	9999.0010000	35	0.2814942
36	0.4047852	37	0.4492188	38	0.0141296	39	0.3088380	40	0.8056641

HS_VIDAR

1	1.9863290	2	0.0614624	3	4.8007820	4	0.1771241	5	0.2006837
6	0.2275391	7	-0.1254884	8	0.2227784	9	0.3747559	10	0.2187501
11	0.0027924	12	0.2000733	13	0.1243897	14	0.0027390	15	0.1231690
16	0.0586853	17	0.0344238	18	-0.0032425	19	4.5468760	20	0.0936890
21	0.0077972	22	-0.0002747	23	0.6015626	24	0.3747559	25	0.0057831
26	0.1711427	27	0.0757446	28	0.0077972	29	0.2534180	30	0.2500001
31	0.0806274	32	0.3215333	33	0.4816895	34	9999.0010000	35	0.2773438
36	0.3981934	37	0.4453126	38	0.0202332	39	0.3210450	40	0.8144532

HS VIDAR

1	1.9863290	2	0.0557251	3	4.8007820	4	0.1777344	5	0.2215577
6	0.2287598	7	-0.1226807	8	0.2193604	9	0.3764649	10	0.2198487
11	0.0060120	12	0.1979981	13	0.1258546	14	0.0065155	15	0.1180421
16	0.0563965	17	0.0347595	18	-0.0006943	19	4.5507820	20	0.0936890
21	0.0077972	22	0.0010910	23	0.6015626	24	0.3747559	25	0.0055542
26	0.1690675	27	0.0765991	28	0.0067596	29	0.2502442	30	0.2507325
31	0.0804443	32	0.3193360	33	0.4792481	34	9999.0010000	35	0.2770997
36	0.3991700	37	0.4519044	38	0.0281372	39	0.3242188	40	0.8139649

HS_VIDAR

1	1.9863290	2	0.0508423	3	4.8007820	4	0.1794434	5	0.2250977
6	0.2294923	7	-0.1218262	8	0.2075196	9	0.3747559	10	0.2226563
11	0.0087280	12	0.1992188	13	0.1262208	14	0.0033569	15	0.1149903
16	0.0596008	17	0.0378418	18	0.0010910	19	4.5546880	20	0.0911255
21	0.0020065	22	0.0025558	23	0.6025391	24	0.3747559	25	0.0029449
26	0.1679688	27	0.0769043	28	0.0075531	29	0.2509766	30	0.2502442
31	0.0800171	32	0.3195802	33	0.4787598	34	9999.0010000	35	0.2592774
36	0.3906251	37	0.4433594	38	0.0015259	39	0.3024903	40	0.7968751

HS VIDAR

1	1.9863290	2	0.0504150	3	4.7968760	4	0.1793214	5	0.2241212
6	0.2285157	7	-0.1218873	8	0.2198487	9	0.3762208	10	0.2224122
11	0.0083618	12	0.2001954	13	0.1267091	14	0.0064392	15	0.1186524
16	0.0587769	17	0.0359802	18	0.0010452	19	4.5546880	20	0.0914307
21	0.0028000	22	0.0016479	23	0.6015626	24	0.3747559	25	0.0035553
26	0.1671143	27	0.0765381	28	0.0072784	29	0.2512208	30	0.2497559
31	0.0806274	32	0.3205567	33	0.4804688	34	-0.1345216	35	0.2580567
36	0.3918458	37	0.4428712	38	0.0252686	39	0.3046876	40	0.8007813

HS VIDAR

Fig. D1 Five scans for position A of truck

			HS VIDAR
CHANNEL	AVERAGE	LOW READING	HIGH READING
1	1.9863290	1.9863290	1.9863290
2	0.0523804	0.0514526	0.0548706
3	4.7968760	4.7968760	4.7968760
4	0.1767823	0.1761475	0.1774903
5	0.2198731	0.2189942	0.2205811
6	0.2276368	0.2270509	0.2285157
7	-0.1244752	-0.1252442	-0.1237183
8	0.2184815	[redacted]	[redacted]
9	0.3805665	0.3791505	0.3823243
10	0.2262696	0.2241212	0.2287598
11	0.0089966	0.0075684	0.0104294
12	0.2025147	0.2009278	0.2041016
13	0.1265870	0.1252442	0.1279298
14	0.0067368	0.0053635	0.0086975
15	0.1179810	0.1172486	0.1193848
16	0.0588623	0.0577698	0.0600891
17	0.0355652	0.0347900	0.0367737
18	0.0009079	-0.0000153	0.0024872
19	4.5515630	4.5507820	4.5546880
20	0.0928100	0.0922241	0.0936890
21	0.0062546	0.0045166	0.0078430
22	-0.0025345	-0.0038528	-0.0013275
23	0.5994141	0.5986329	0.6000977
24	0.3747559	0.3747559	0.3747559
25	0.0029953	0.0015030	0.0050354
26	0.1644532	0.1634522	0.1665040
27	0.0745850	0.0738525	0.0759277
28	0.0050781	0.0043335	0.0060425
29	0.2486817	0.2480469	0.2495118
30	0.2476563	0.2465821	0.2490235
31	0.0797485	0.0792236	0.0805054
32	0.3201172	0.3198243	0.3208009
33	0.4774903	0.4765626	0.4787598
34	-0.1237794	-0.1248780	-0.1226807
35	0.2762208	[redacted]	[redacted]
36	0.4038087	0.3999024	0.4094239
37	0.4528321	0.4487305	0.4577637
38	0.0308716	[redacted]	[redacted]
39	0.3208985	0.3171387	0.3278809
40	0.8236329	0.8212891	0.8261719

Fig. D2 Average off position data

Consider gaged section I on the main girder. Only gages 1, 2 and 3 will be used. These gages correspond to channels 2, 3 and 4 respectively.

	Ch. 2	Ch. 3	Ch. 4
Average reading for north end off position, from Fig. D2	0.05238	4.79688	0.17678
Scan one reading for position A of truck, from Fig. D1	0.03140	4.77344	0.19470
Average off--individual scan	0.02098	0.02344	-0.01792

These are reduced voltages due to the truck loading at position A, in gages 1, 2 and 3. It has been proven that there is no composite action between the girder and the deck slab, i.e., the neutral axis is at the center of the girder cross-section. Hence gages 1, 2 and 3 can be averaged to get the average voltage.

Average voltage at position A = (gage 1 + gage 2 - gage 3)/3

= 0.02078 volts.

Using the relationship shown in Appendix B,

Strain = (2.0/bridge voltage) x (channel voltage/400)

Hence stress = (2.0/1.98633) x (0.02078/400) x 29,000

= 1.517 ksi

The section modulus of gaged I being 2560 in^3, the moment corresponding to this stress is 1.517 x 2560 = 3883 k-in.

This moment has been plotted on the dynamic data for gages 1, 2 and 3, shown in Fig. D3. Similarly moment values for scans 2-5 were found and also plotted. This has been repeated for the other three gaged moment sections and two reaction hanger supports. The same process has been followed for truck location B, i.e. rear axle 35 feet from south end support. The results are plotted in Fig. D3-D8.

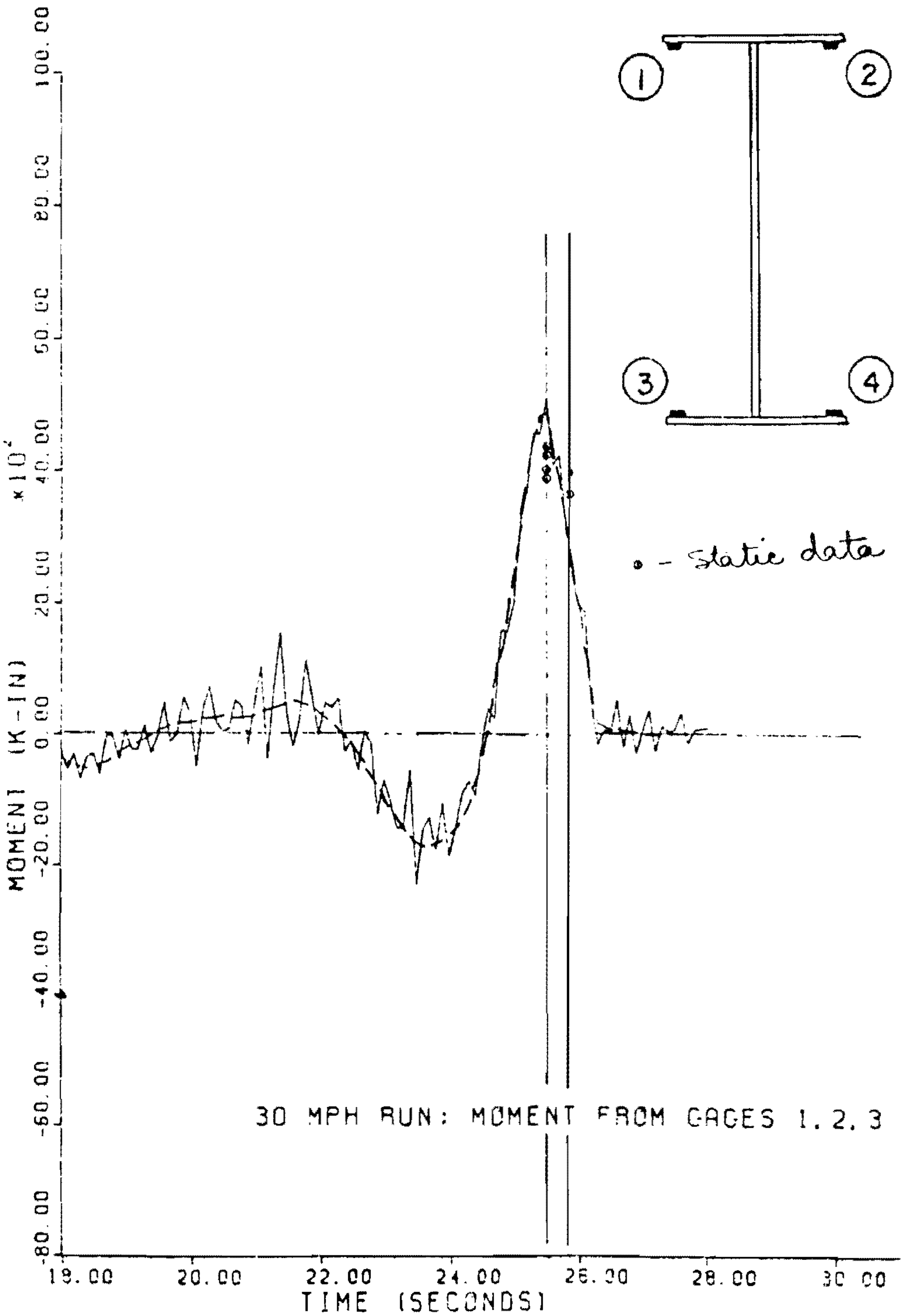

Fig. D.3 30 mph run: moment from gages 1, 2, 3

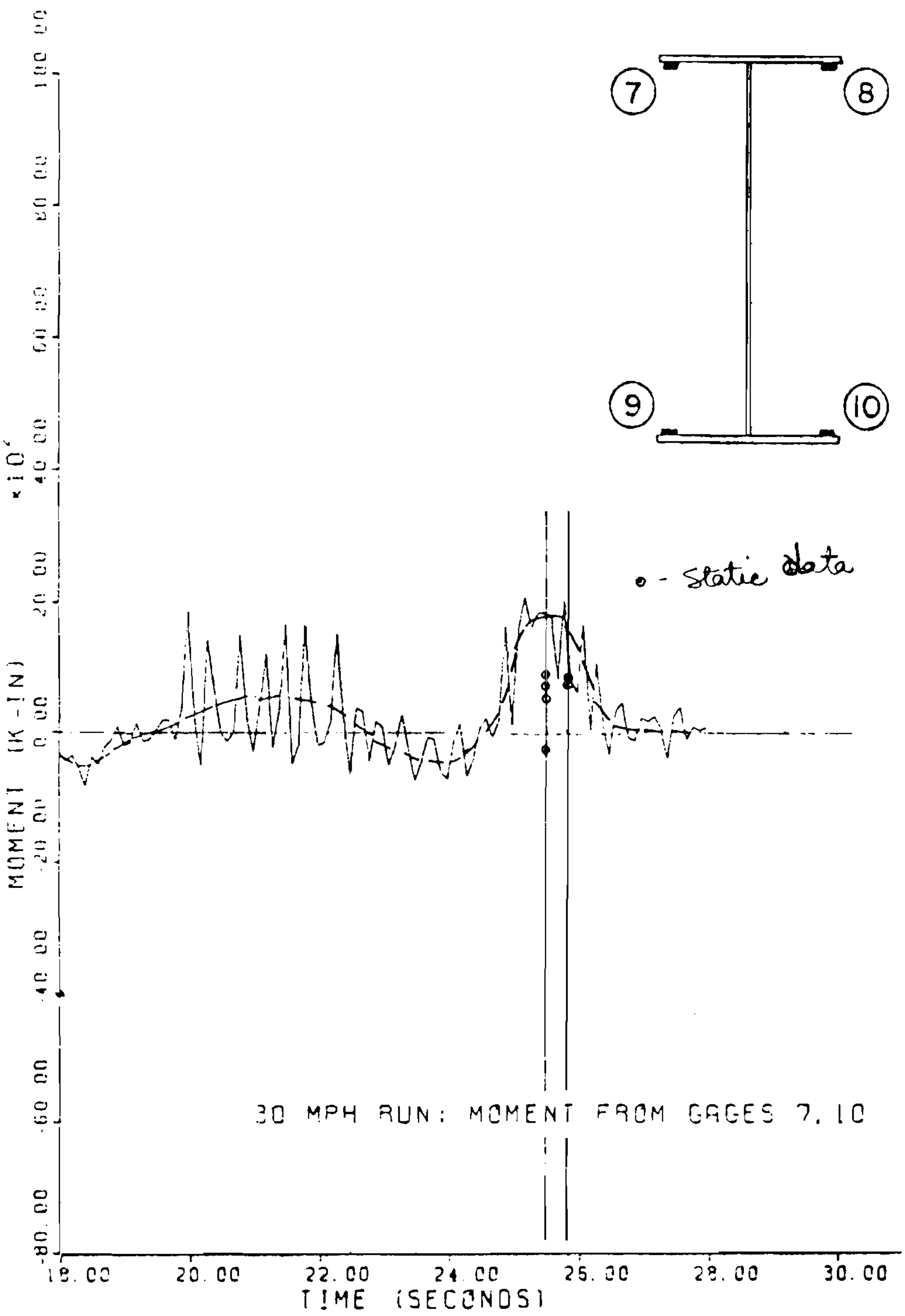

Fig. D.4 30 mph run: moment from gages 7, 10

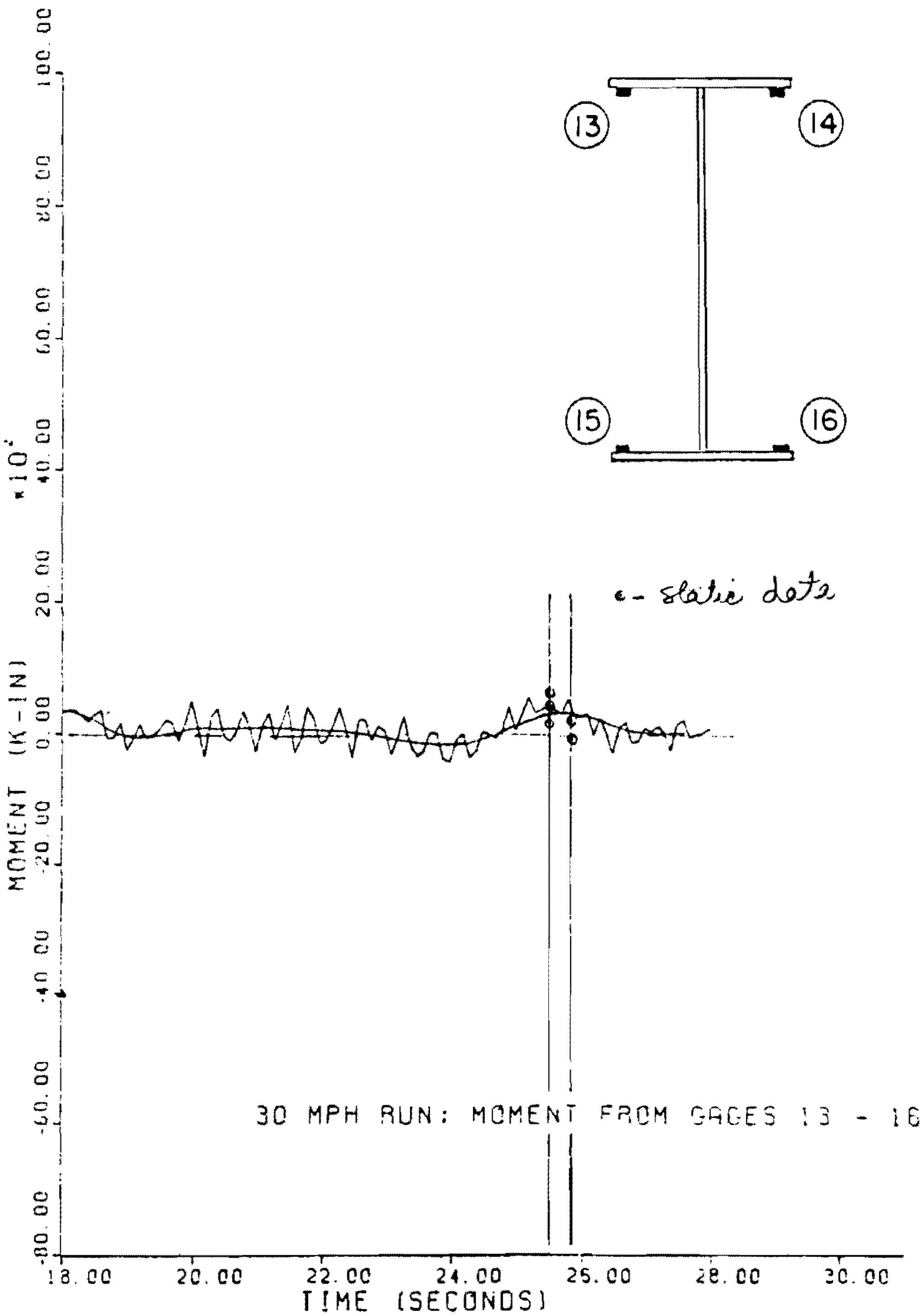

Fig. D.5 30 mph run: moment from gages 13-16

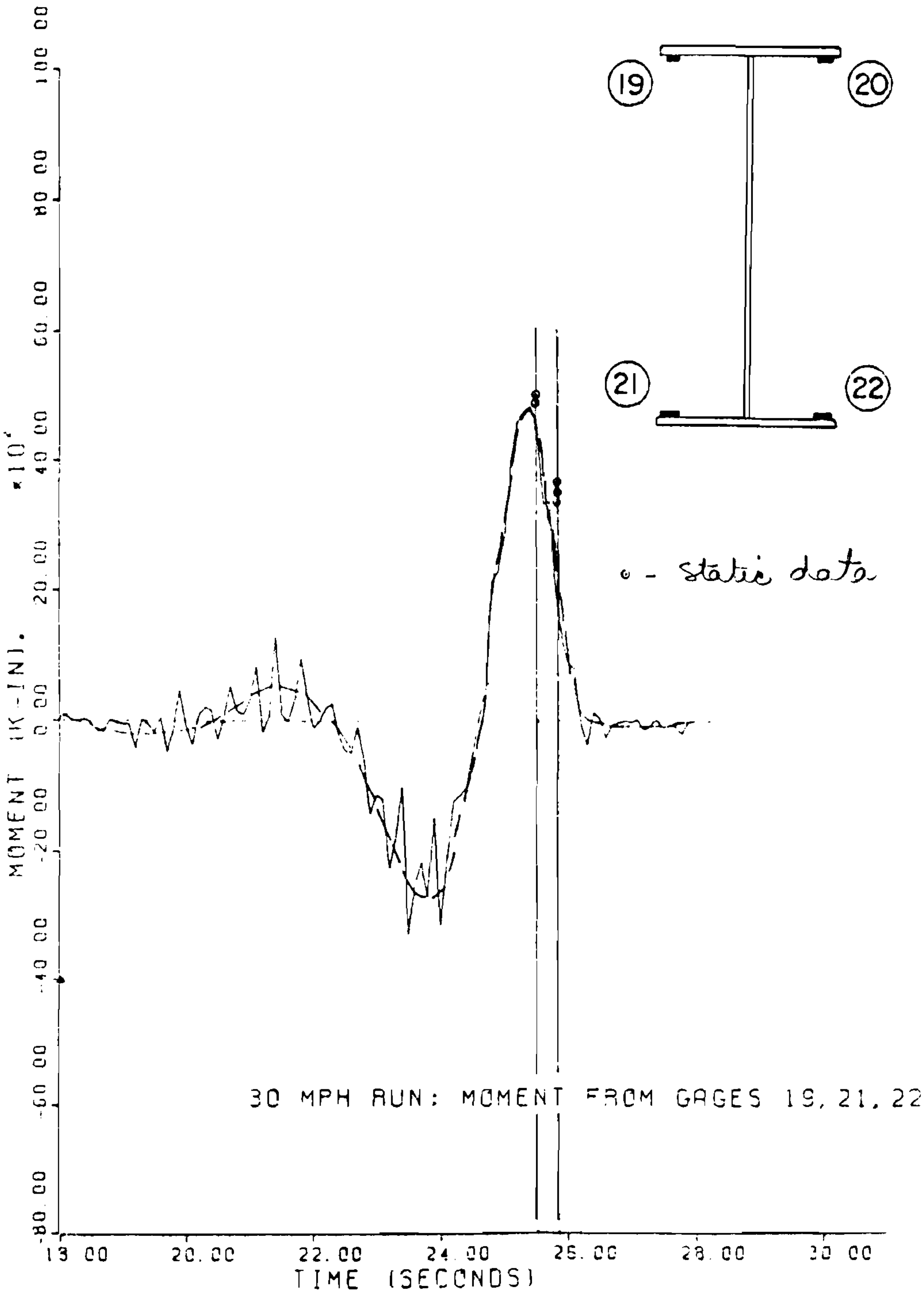

Fig. D.6 30 mph run: moment from gages 19, 21, 22

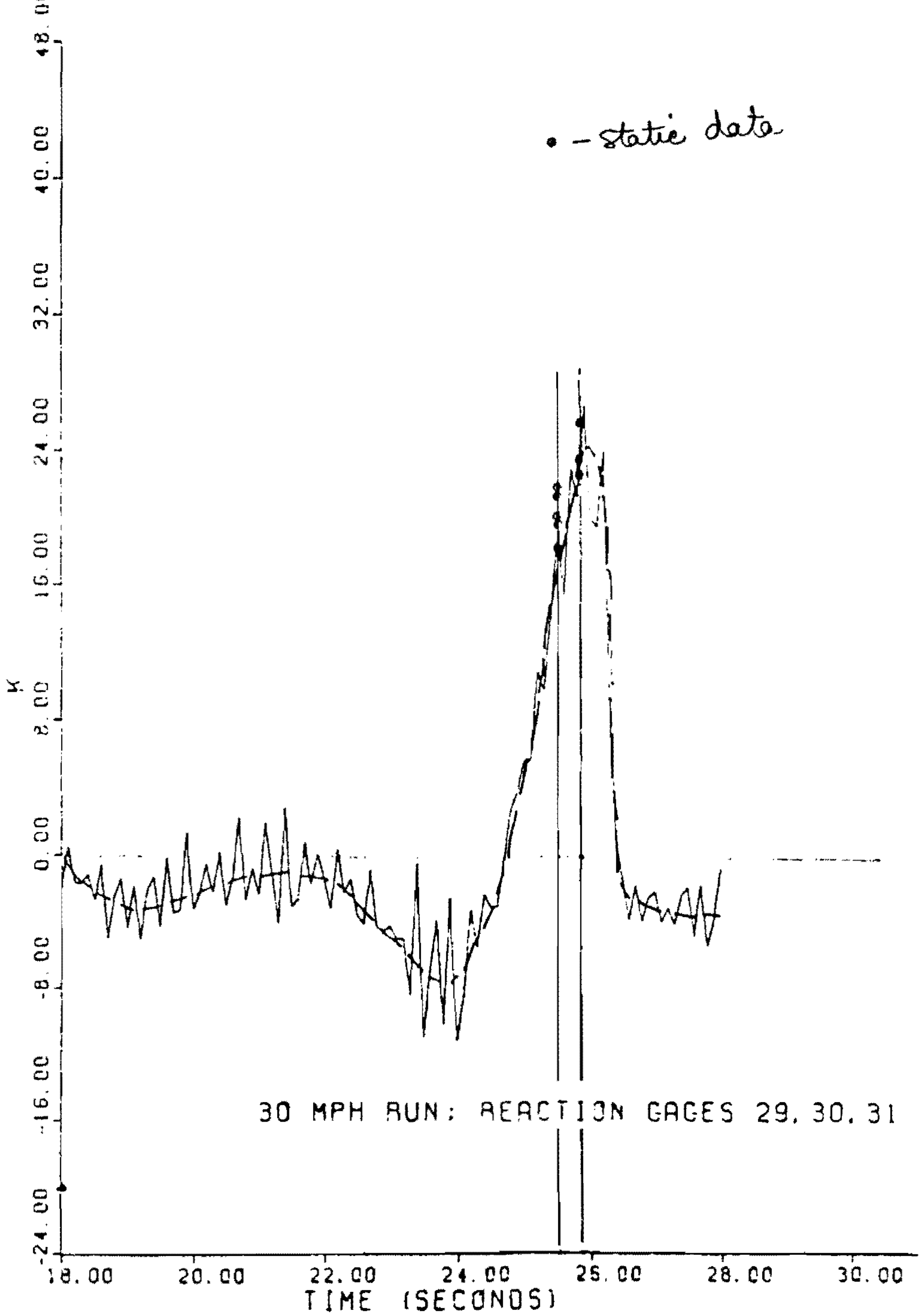

Fig. D.7 30 mph run: reaction gages 29, 30, 31

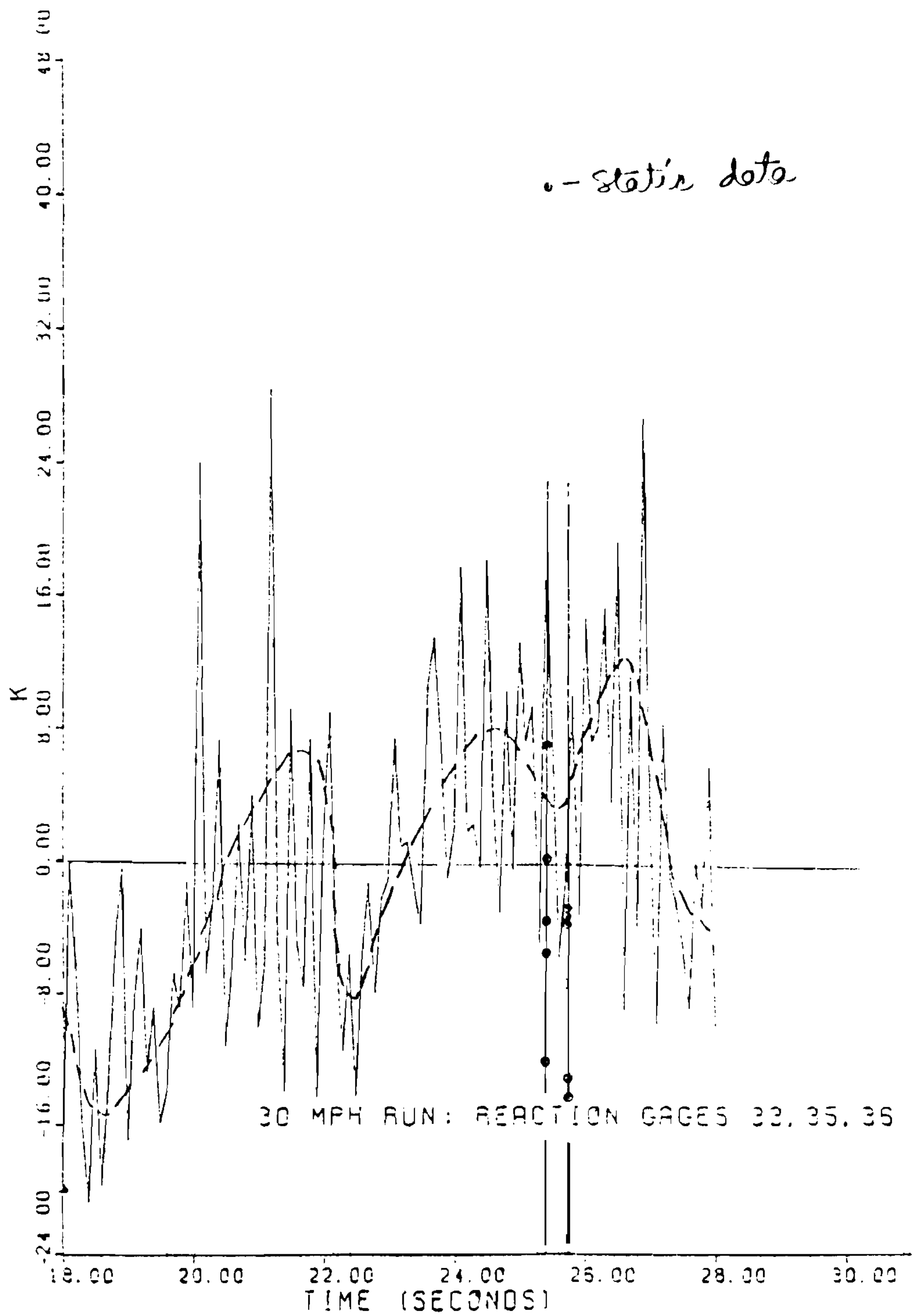

Fig. D.8 30 mph run: reaction gages 33, 35, 36

A P P E N D I X   E

DYNAMIC DATA REDUCTION

APPENDIX E

DYNAMIC DATA REDUCTION

Three truck positions were chosen to compare the dynamic data with the analytical results.

(a) The rear axle of the truck 28 feet from the south end support.

(b) The rear axle of the truck 42 feet from the south end support.

(c) The rear axle of the truck 42 feet from the second last south support.

For the 30 mph run, the truck positions correspond to scans number 257, 254 and 237 respectively. Since the scanning rate was 0.1 secs, these scans were made at 25.7 secs, 25.4 secs and 23.7 secs respectively, after the start of the run. The moment and the reaction plots are shown in Fig. E1-E6. The measured values that were read off these plots are shown in Table E1.

Static Equilibrium Check

Using the elastic properties of the slab, the frame program calculates the truck load distribution among the cross-beams. These beams then transfer the load to the girders. Since the distribution of load among the two girders was not known, they were idealized as one girder. The moment at a gaged section for this idealized girder was taken as a sum of the corresponding moments from both the girders. Knowing the load and the moment, the reaction was calculated by ensuring static equilibrium, as shown in the sample calculations.

This reaction compares very well with the measured and the analytically predicted reaction, for the first two positions of the truck. For the third position of the truck, i.e. on the

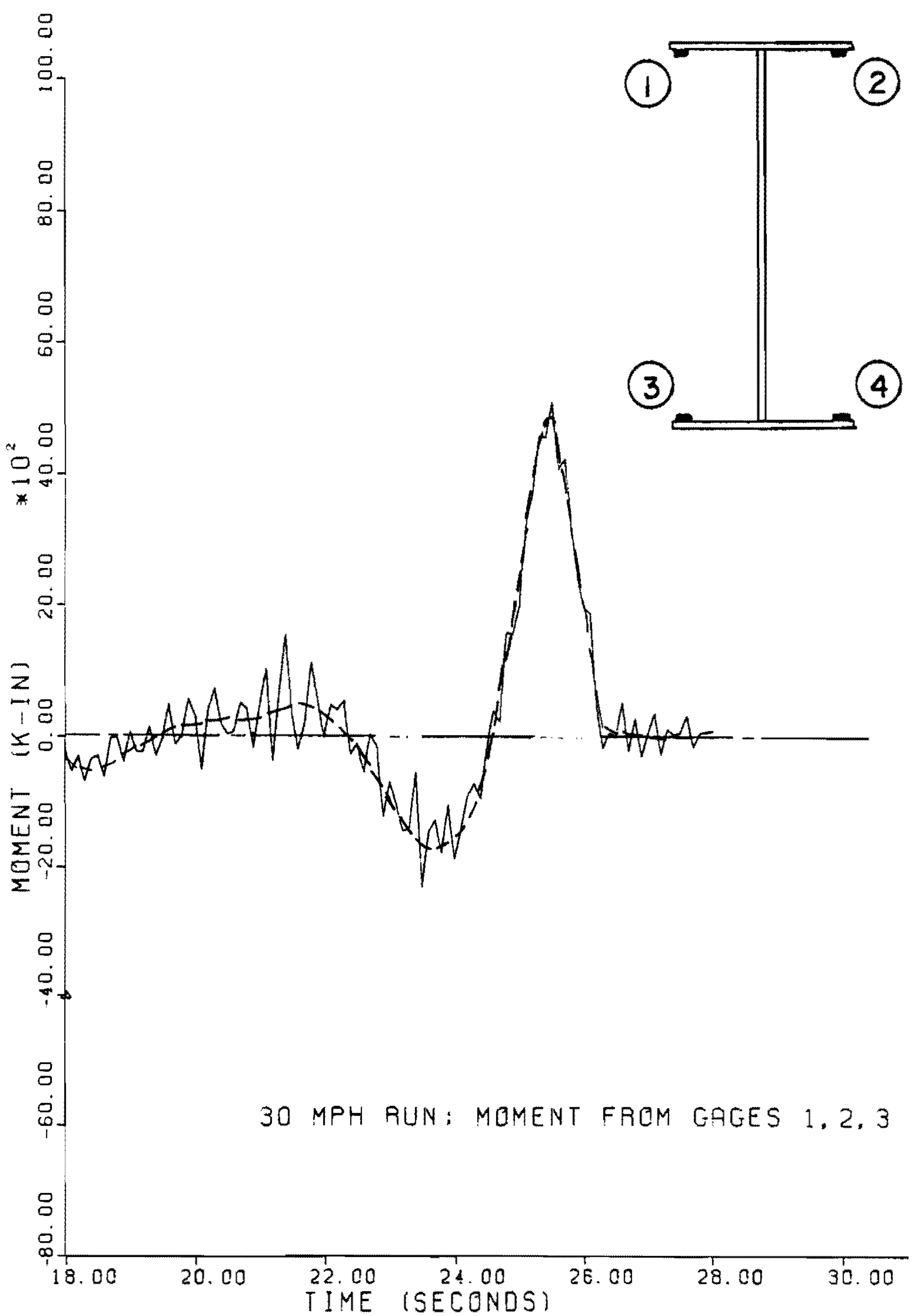

Fig. E.1 30 mph run: moment from gages 1, 2, 3

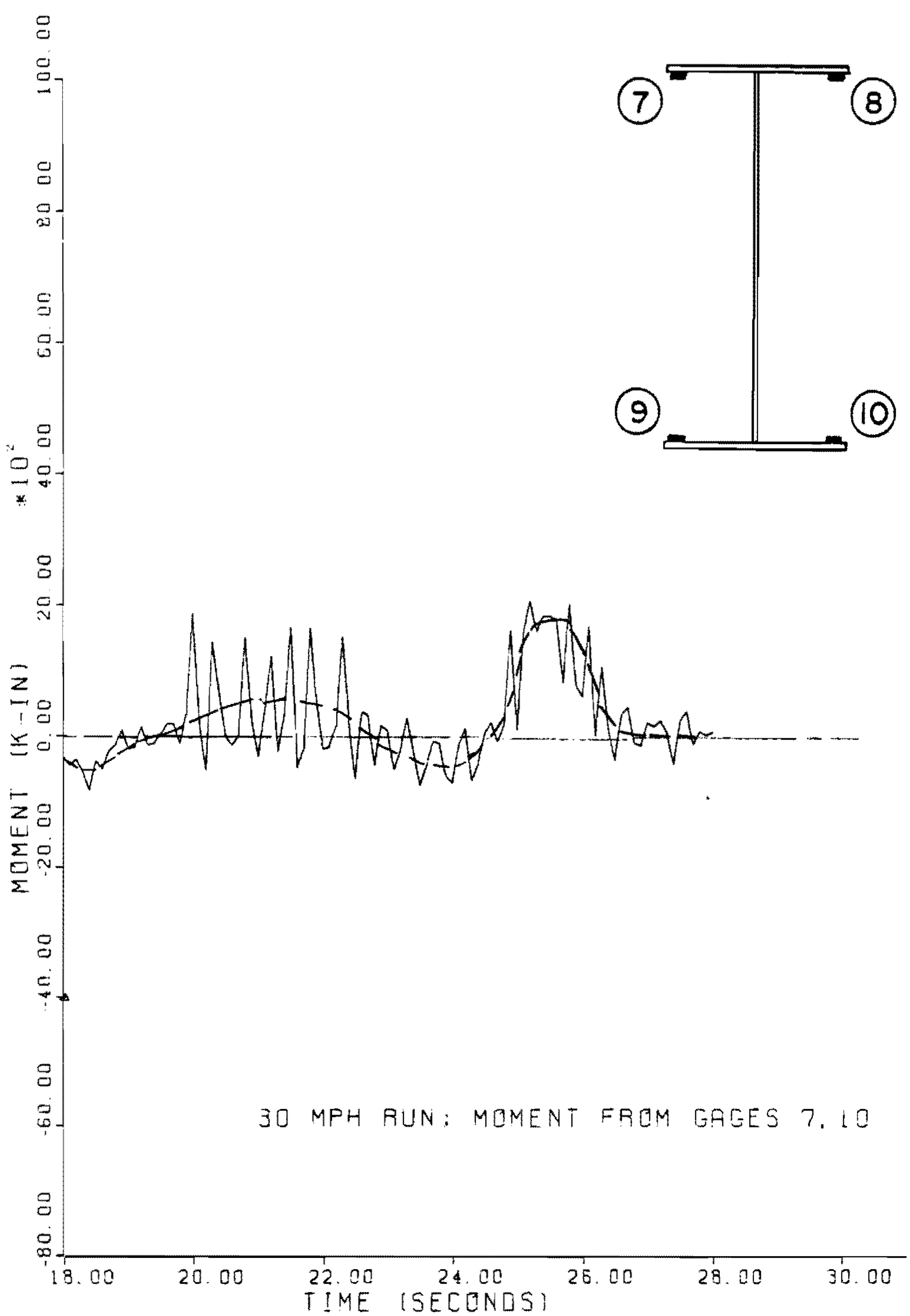

Fig. E.2 30 mph run: moment from gages 7, 10

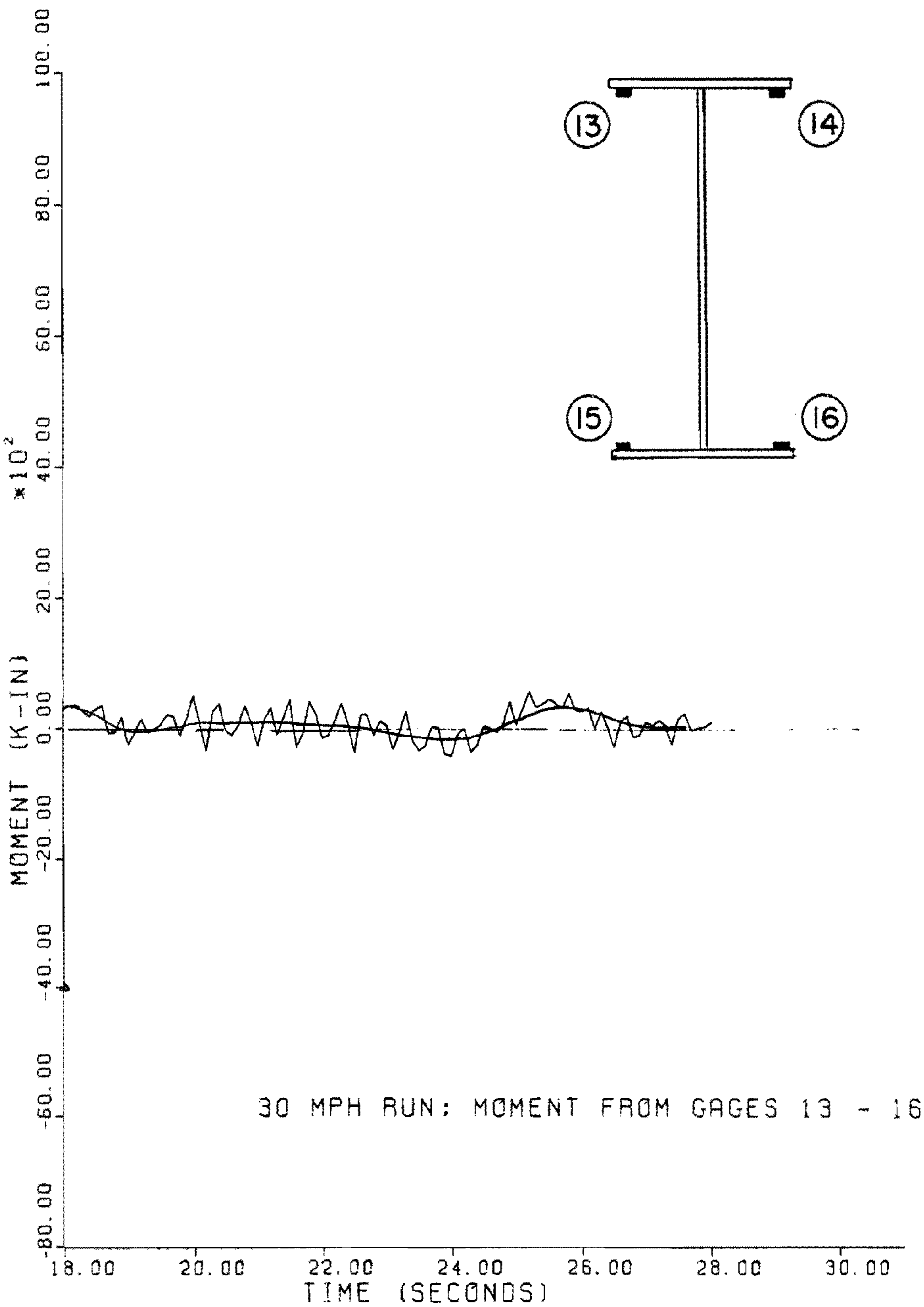

Fig. E.3 30 mph run: moment from gages 13-16

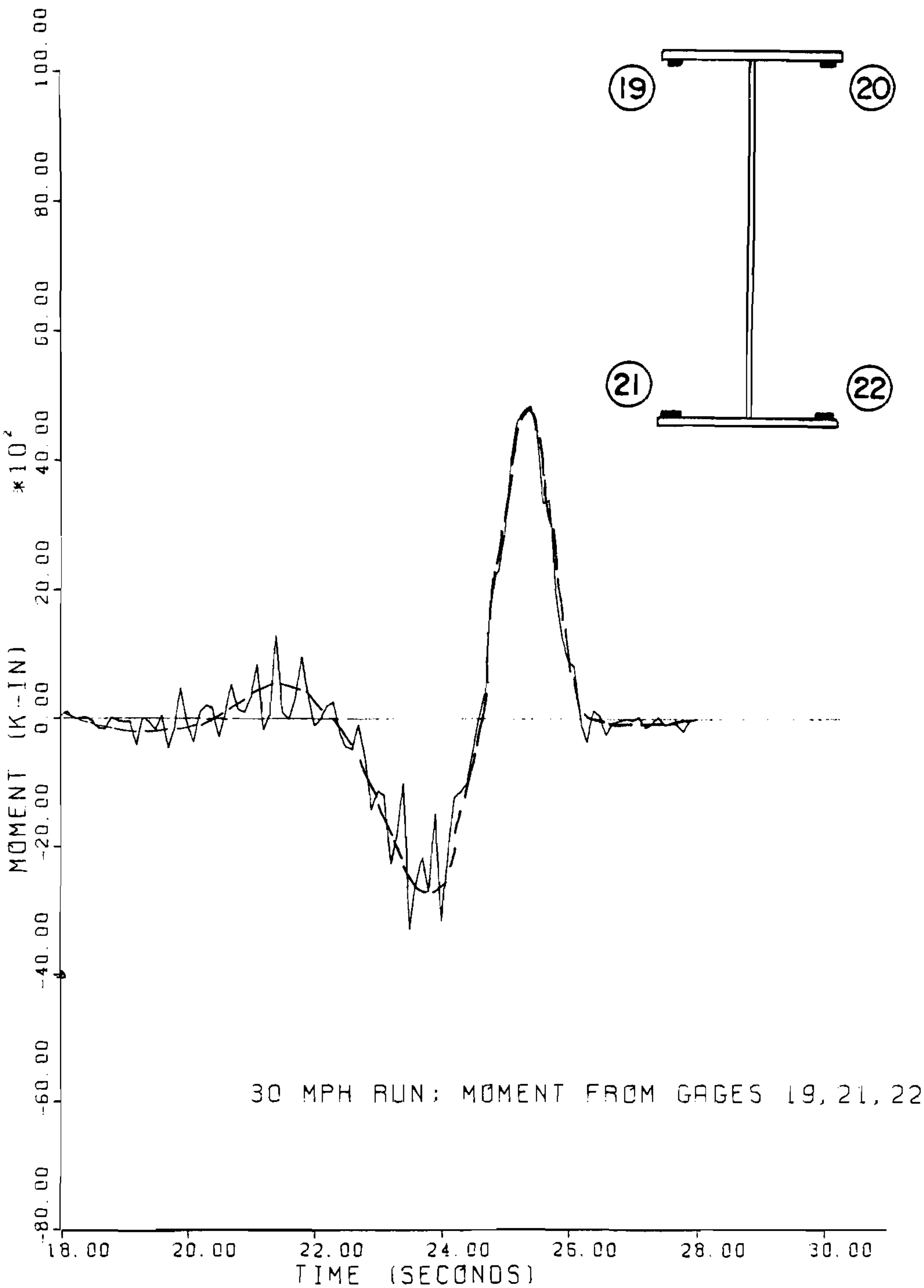

Fig. E.4 30 mph run: moment from gages 19, 21, 22

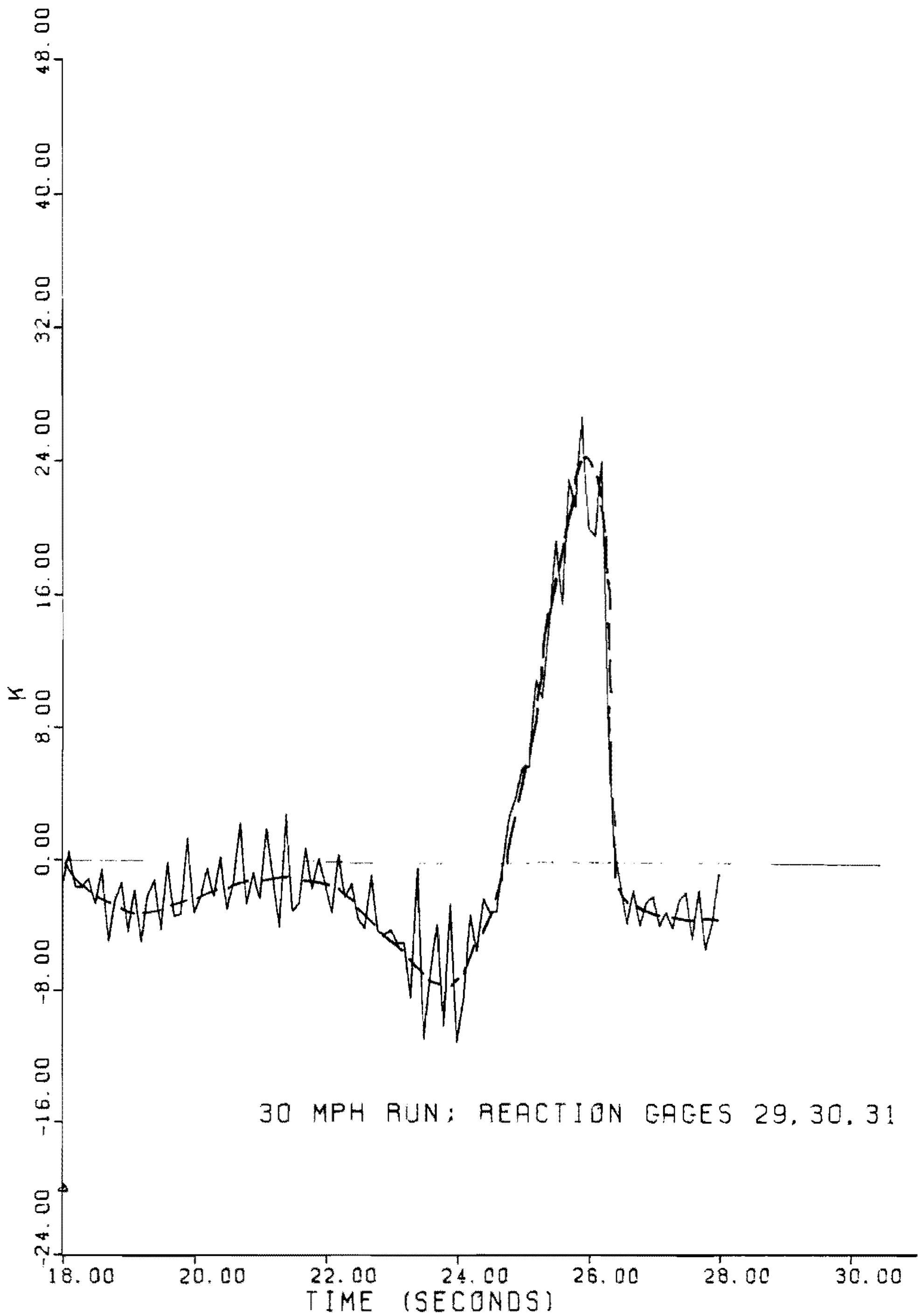

Fig. E.5 30 mph run: reaction gages 29, 30, 31

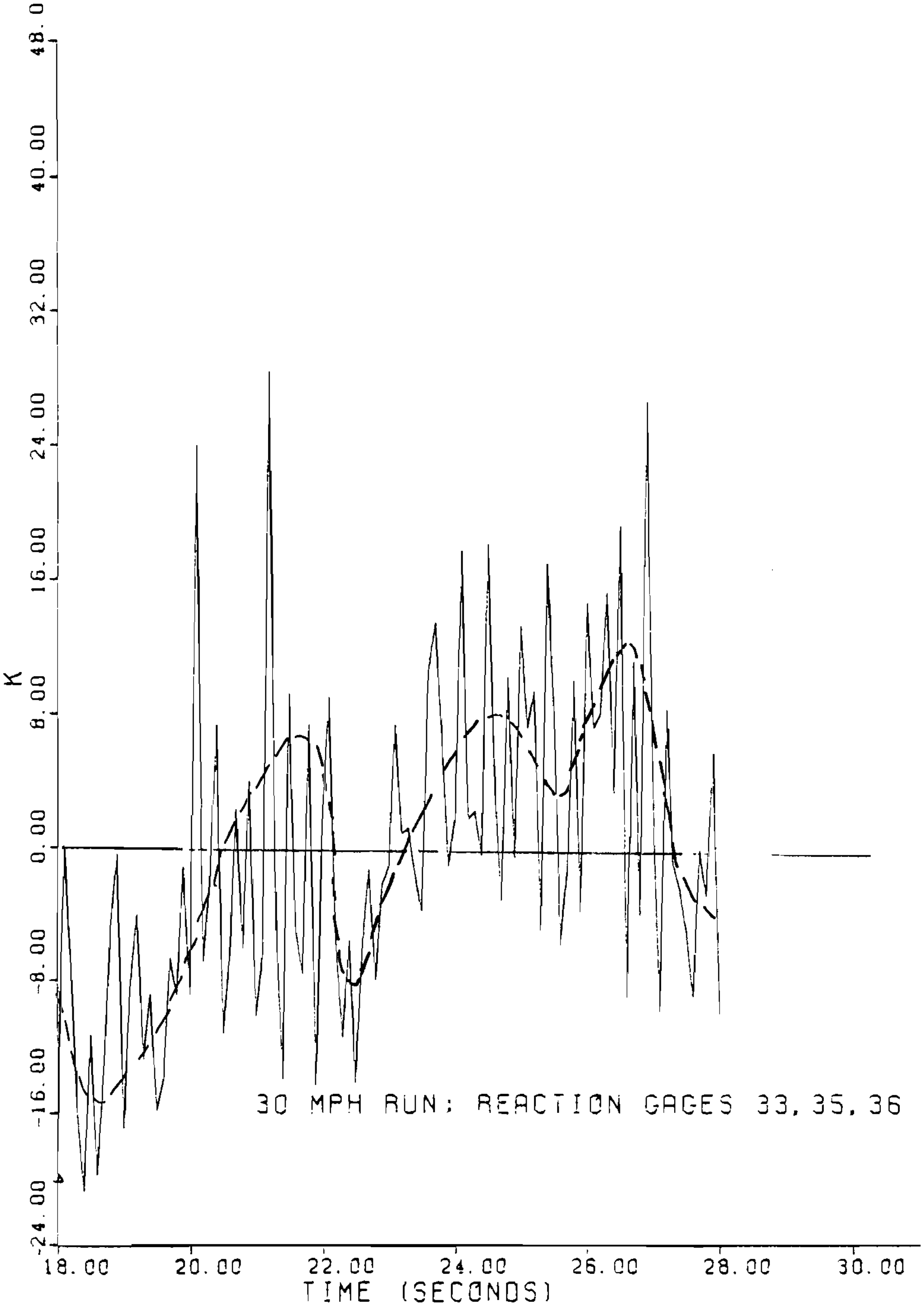

Fig. E.6 30 mph run: reaction gages 33, 35, 36

TABLE E1 30 MPH RUN--MEASURED VARIABLES

Truck Location	Measured Variable	Main Girder	Other Girder
28' from south end support	Moment at section I (k-in)	3825	1600
	Moment at section II (k-in)	2870	750
	Reaction from hanger (k)	21.5	8.0
40' from south end support	Moment at section I (k-in)	4950	1850
	Moment at section II (k-in)	4800	870
	Location from hanger (k)	13.9	5.8
42' from second-last support	Moment at section I (k-in)	-1550	-370
	Moment at section II (k-in)	-2450	-450
	Reaction from hanger (k)	-7	+6

Sample Calculation

30 mph run, 28' from south end support

Moment at Gage Section I, main girder = 3825 k-in.
Moment at Gage Section I, other girder = 1600 k-in.
Combined moment at Gage Section I = 5425 k-in.

$$R \times 28.33 = (5425/12) + (1.37 \times 26.25) + (26.7 \times 12.5)$$
$$= 821.8 \text{ k-ft}$$

$$R = 29.0 \text{ kips}$$

Moment at Gage Section II, main girder = 2870 k-in.
Moment at Gage Section II, other girder = 750 k-in.
Combined moment at Gage Section II = 3620 k-in.

$$R \times 39.83 = (3620/12) + (1.37 \times 37.75) + (26.7 \times 24)$$
$$+ (28.97 \times 6) = 1168.1 \text{ k-ft}$$

$$R = 29.32 \text{ kips}$$

Measured Reaction = 29.5 kips

Analytically Predicted Reaction = 31.9 kips second span, the effect of the other traffic on the first span is very large, hence the measured values show a larger discrepancy.

Similarly for the 5 mph run, the truck positions correspond to scans number 70, 86 and 181 respectively. These scans were made at 7.0, 8.6 and 18.1 secs respectively, after the start of the run. The moments and the reaction plots are shown in Fig. E7-E12. The measured values, that were read off these plots are shown in Table E2. By ensuring static equilibrium, the reactions were again calculated and found to be in good agreement with the analytically predicted reactions. This proves the validity of the measured moments. However, the measured reactions are larger than the statically determined ones because of the presence of other traffic on the other girder.

This process was not repeated on the 50 mph run data, since the data collected for the two earlier runs was found in agreement with static equilibrium. The reaction gages were therefore not used for this run. The data is attached in Fig. E13-E16.

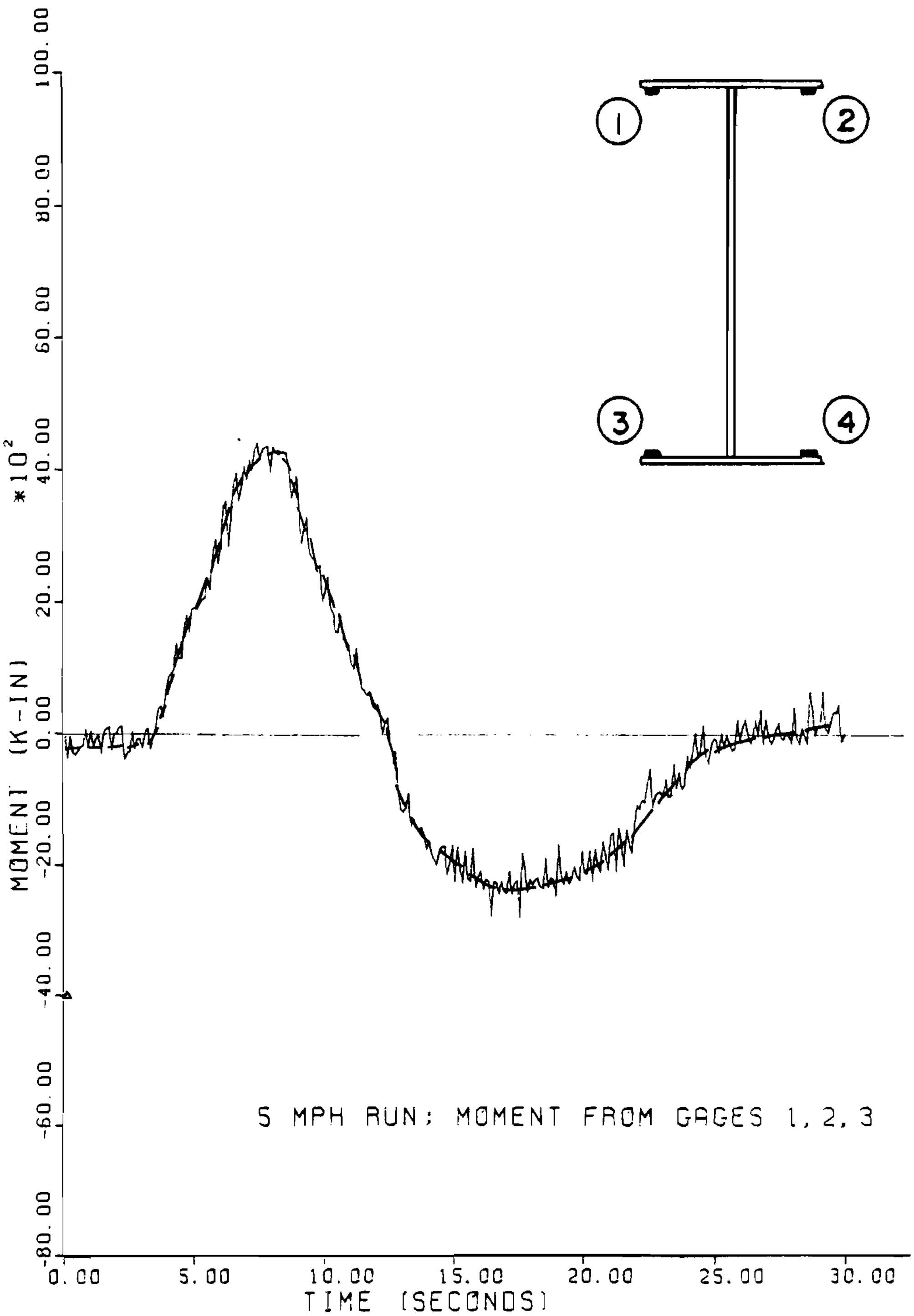

Fig. E.7 5 mph run: moment from gages 1, 2, 3

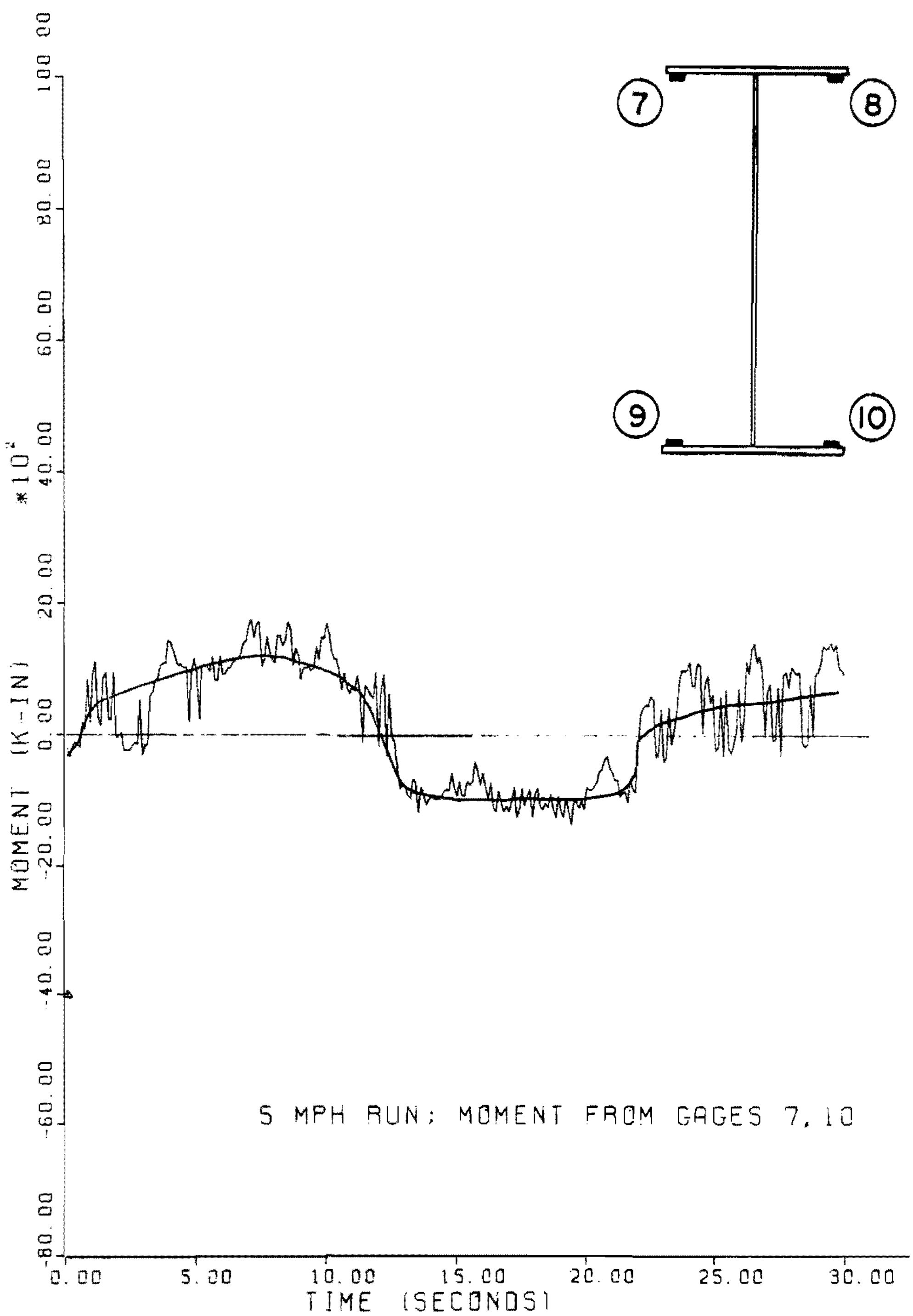

Fig. E.8 5 mph run: moment from gages 7, 10

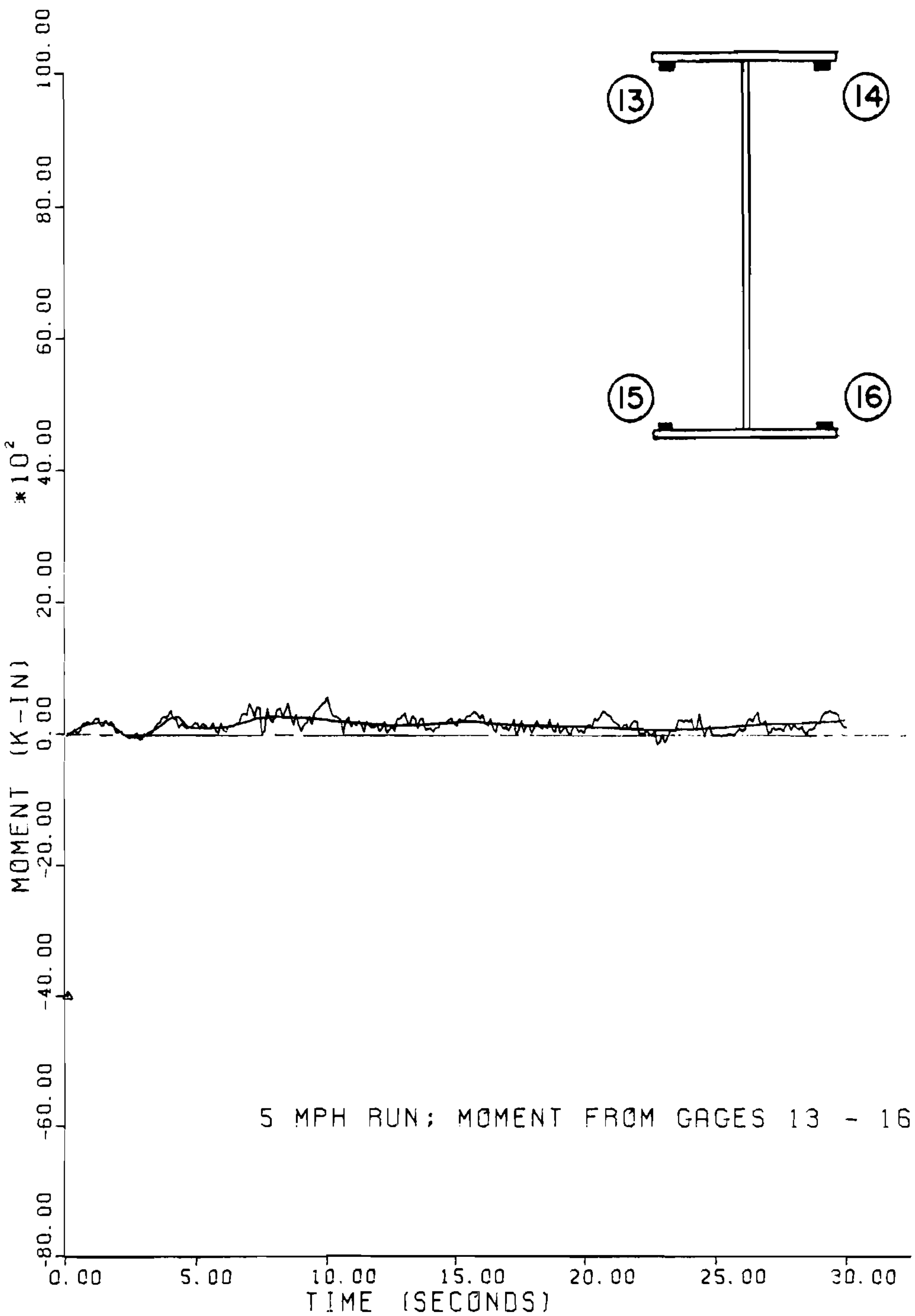

Fig. E.9 5 mph run: moment from gages 13-16

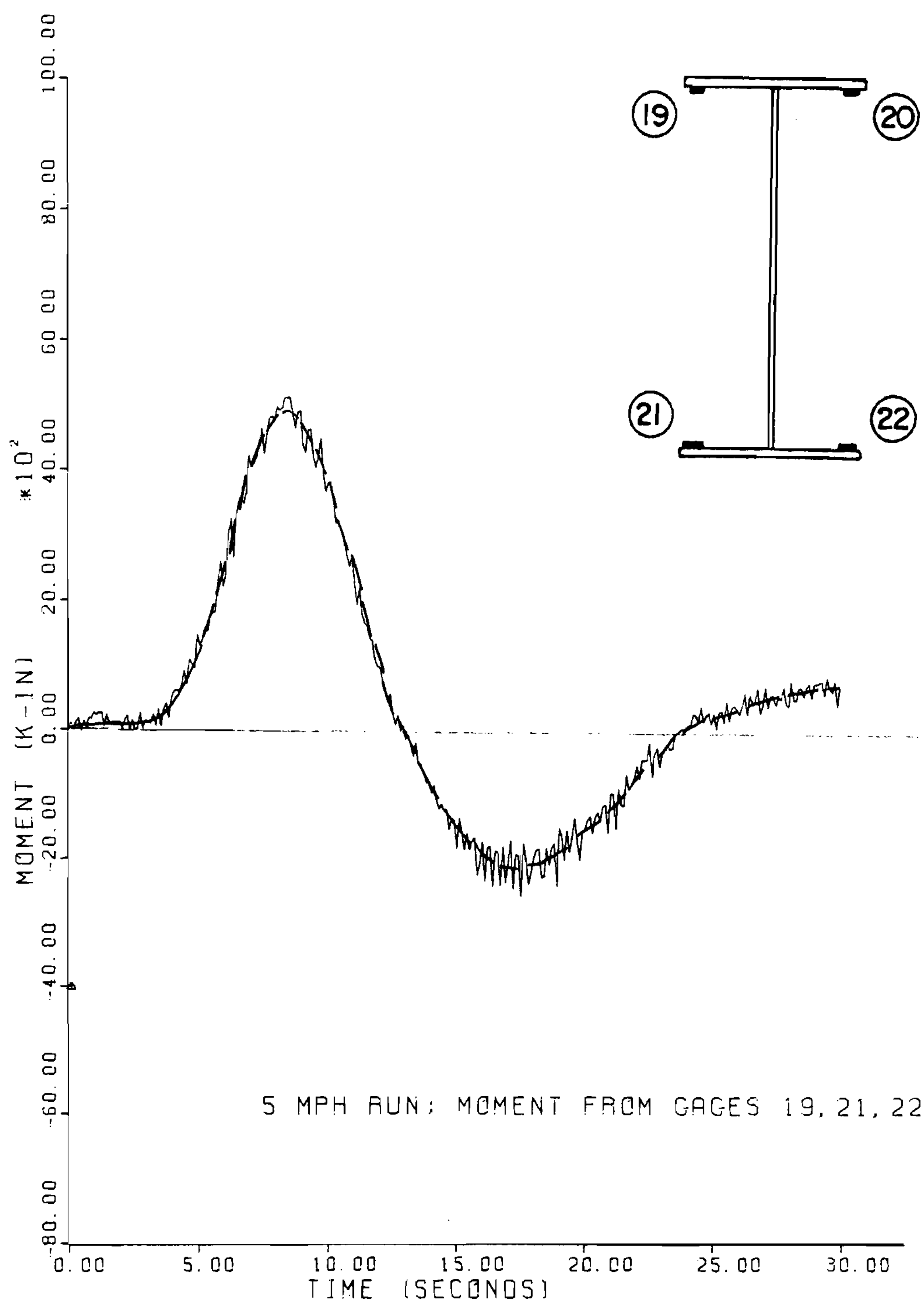

Fig. E.10 5 mph run: moment from gages 19, 21, 22

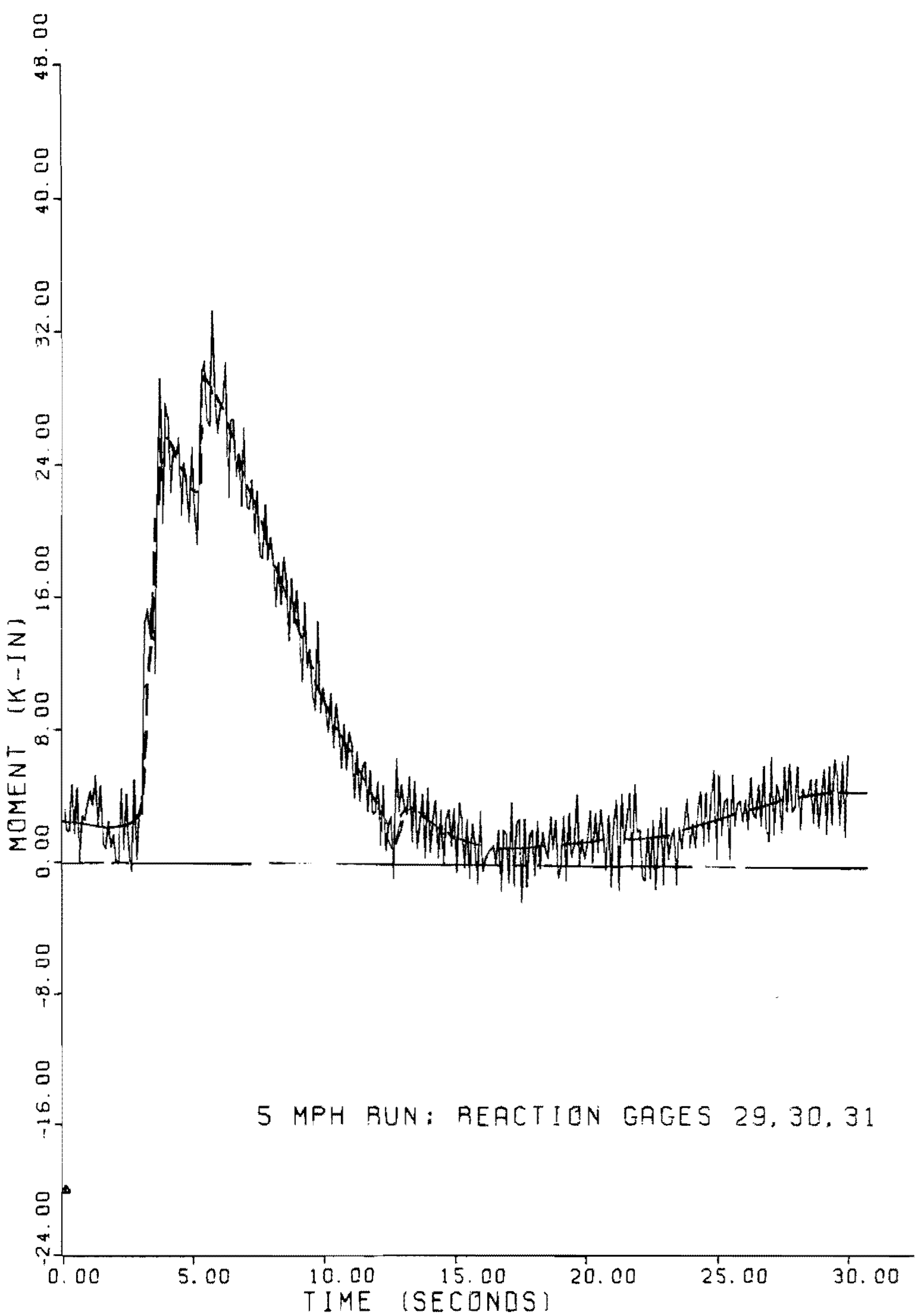

Fig. E.11 5 mph run: reaction gages 29, 30, 31

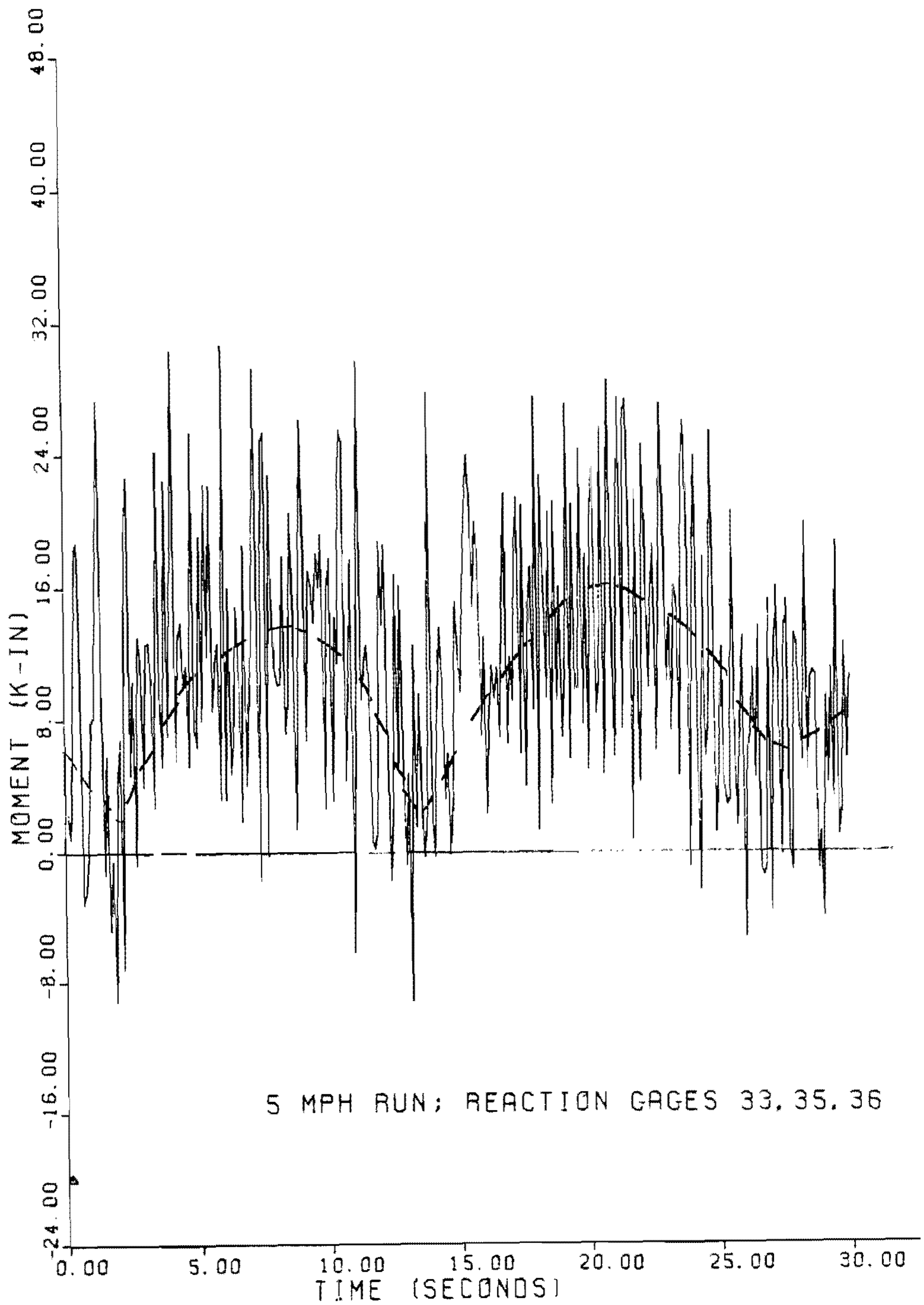

Fig. E.12 5 mph run: reaction gages 33, 35, 36

TABLE E2 5 MPH RUN--MEASURED VARIABLES

Truck Location	Measured Variable	Main Girder	Other Girder
28' from south end support	Moment at section I (k-in)	3890	1325
	Moment at section II (k-in)	3930	620
	Reaction from hanger (k)	23.9	14.0
40' from south end support	Moment at section I (k-in)	4032	1400
	Moment at section II (k-in)	5110	780
	Reaction from hanger (k)	17.0	15.9
42' from second last support	Moment at section I (k-in)	-2215	-1000
	Moment at section II (k-in)	-2000	-160
	Reaction from hanger (k)	+1.0	+14.0

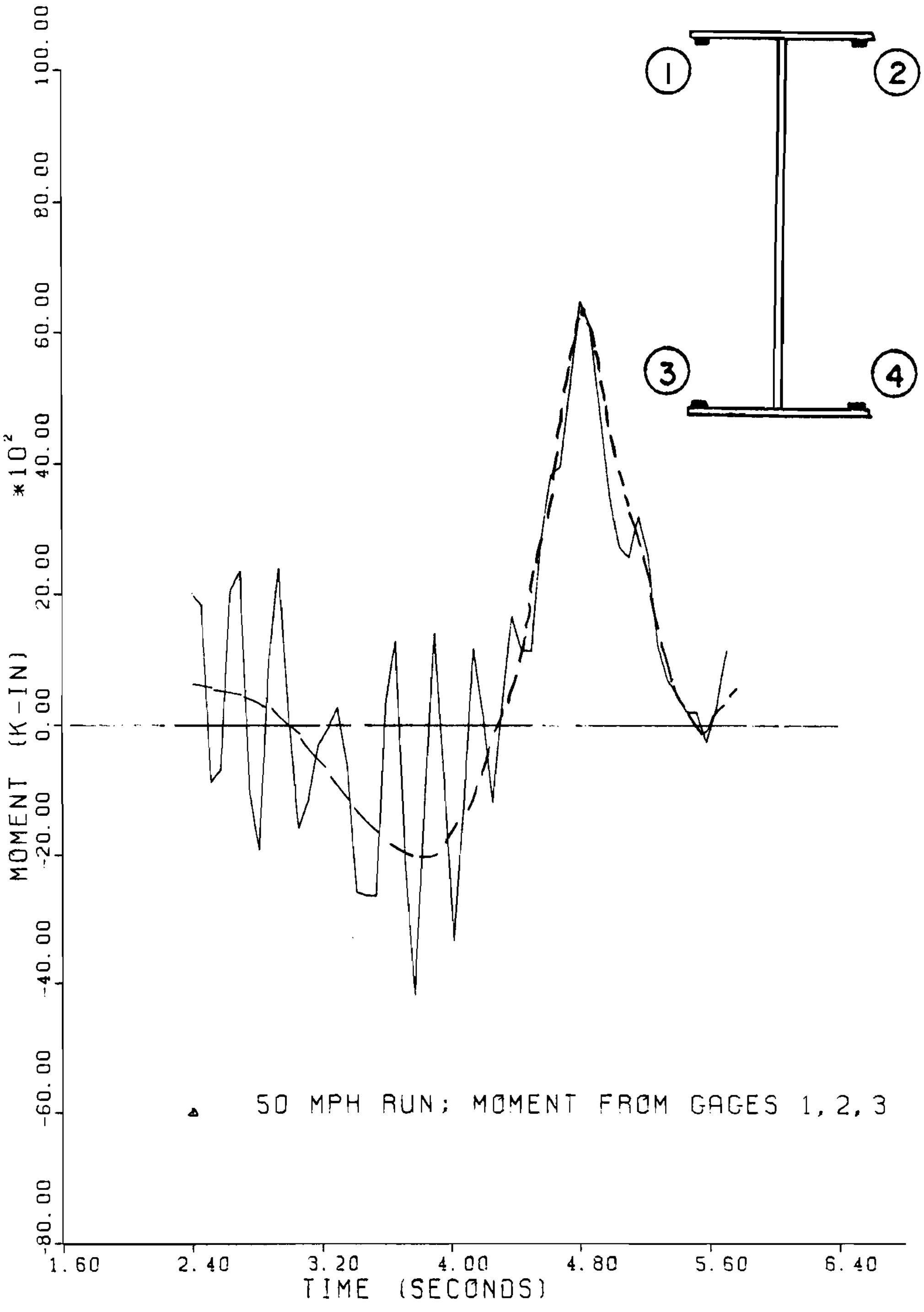

Fig. E.13 50 mph run: moment from gages 1, 2, 3

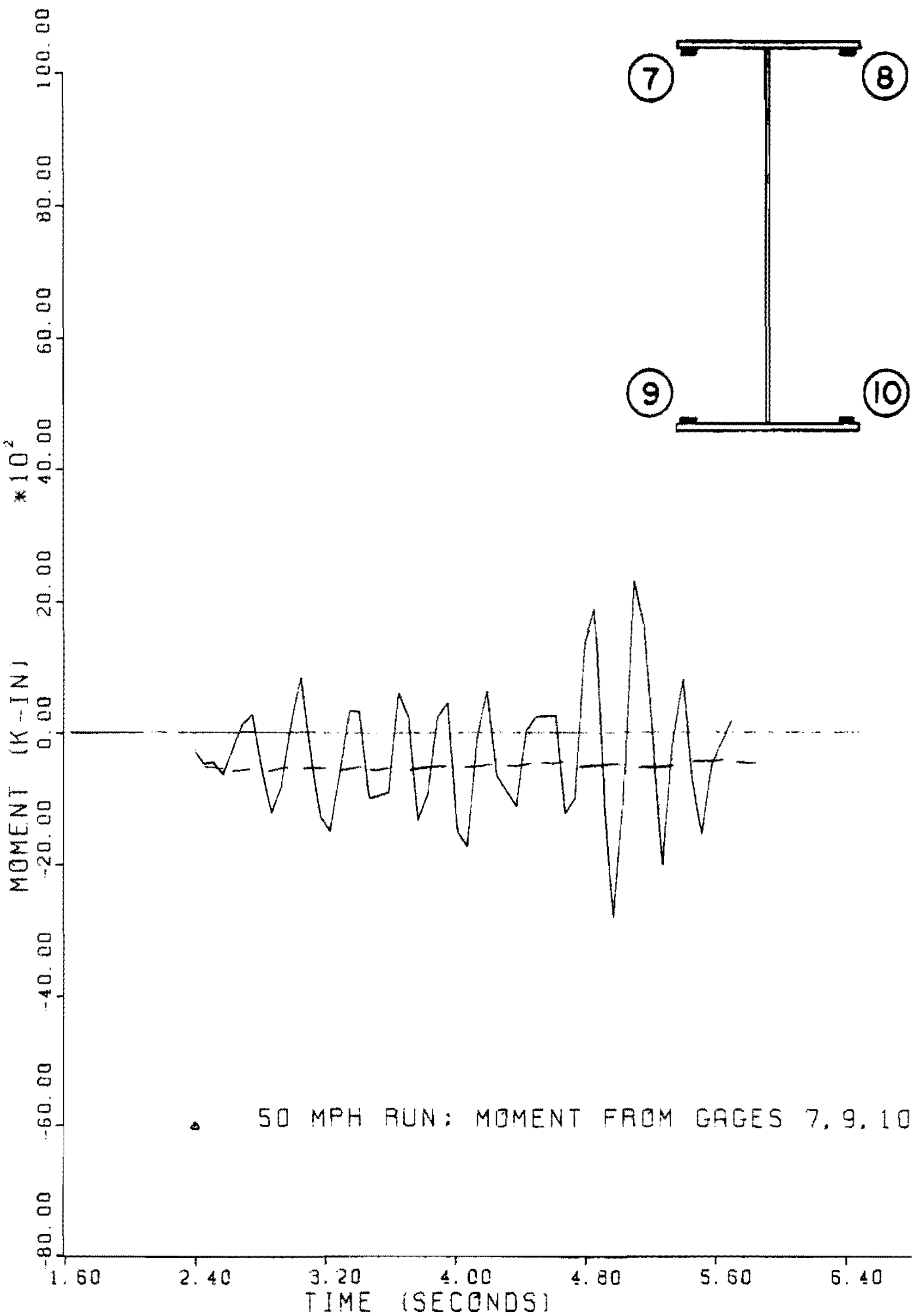

Fig. E.14 50 mph run: moment from gages 7, 9, 10

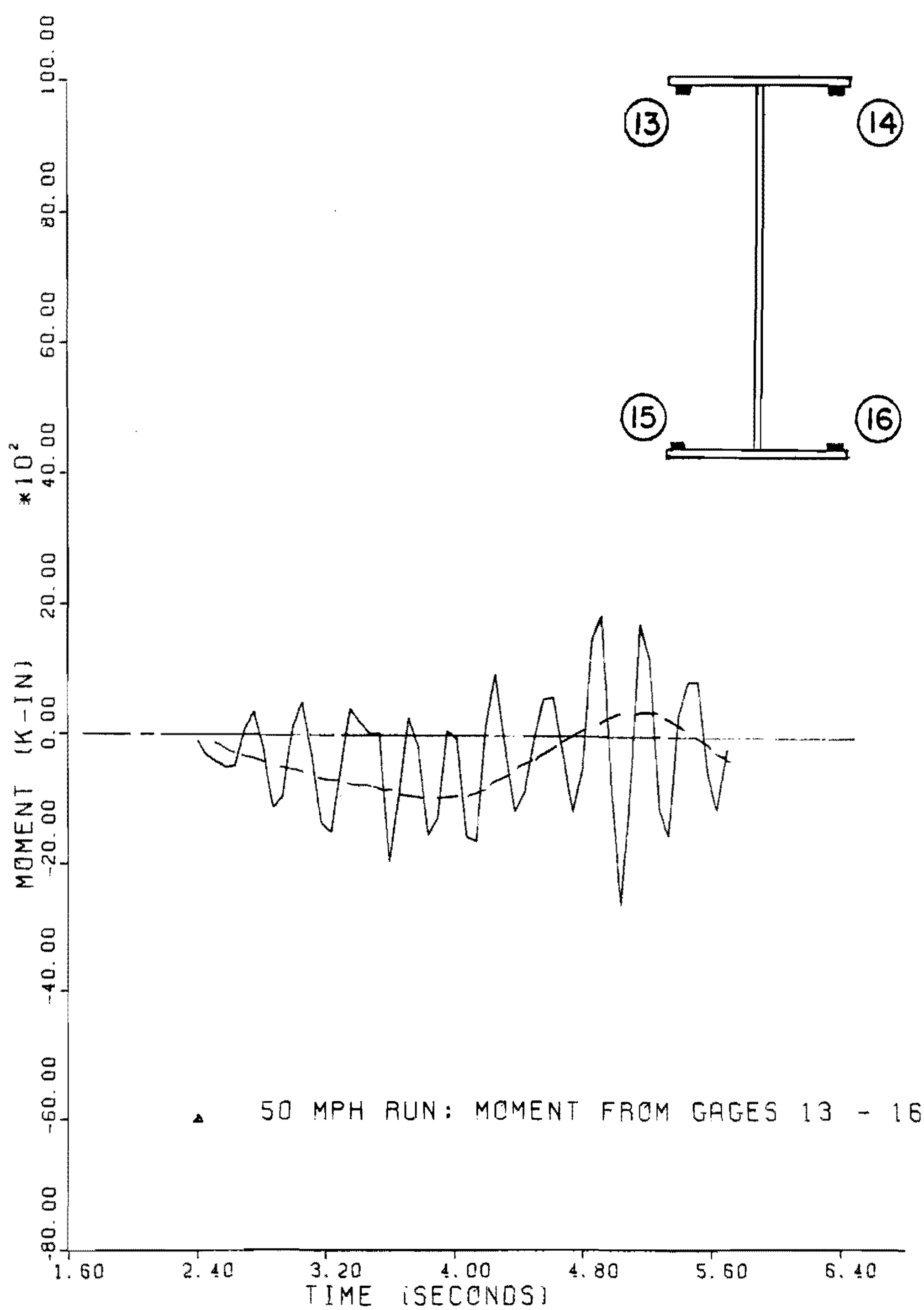

Fig. E.15 50 mph run: moment from gages 13-16

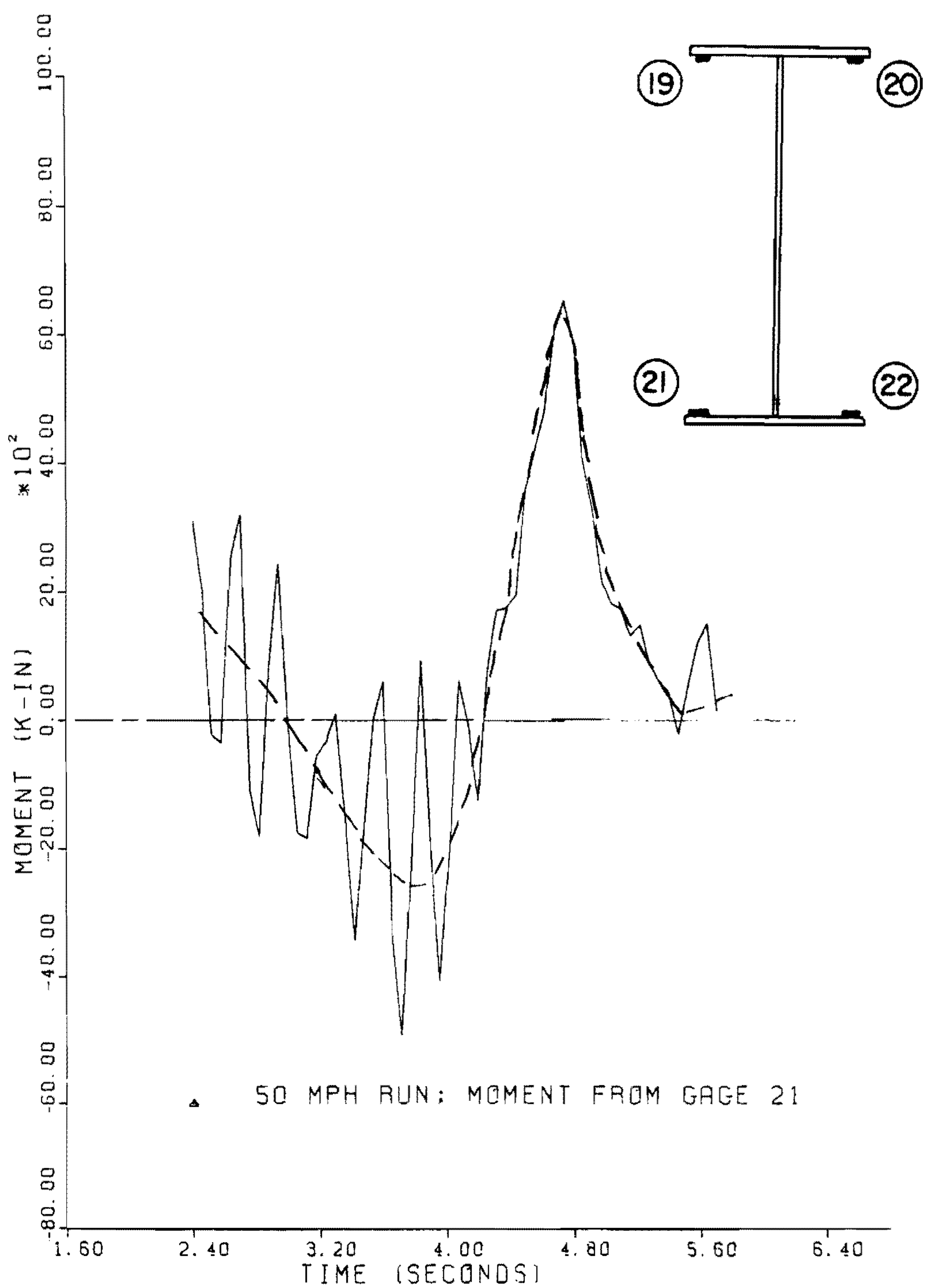

Fig. E.16 50 mph run: moment from gage 21